A PERSONAL OVERVIEW OF THE DEVELOPMENT OF PATCH ANTENNAS

Part 1

Kai Fong Lee

Dean Emeritus, School of Engineering and Professor Emeritus, Electrical Engineering, University of Mississippi

and

Professor Emeritus, Electrical Engineering, University of Missouri-Columbia

October 28, 2015

City University of Hong Kong

Abstract

This four-hour talk is a personal account of the development of microstrip patch antennas. It begins with how the speaker, with a background in theoretical plasma physics, got into the study of patch antennas in the early 1980's. After a review of basic theory, the speaker's involvement in the development of patch antenna design through research on various topics is described. These include basic characteristics, broadbanding and size-reduction techniques, full wave analysis, dual and triple band designs, circularly polarized as well as reconfigurable patch antennas. Highlighted in the presentation is the close collaboration with the Department of Electronic Engineering at the City University of Hong Kong through the years. The talk ends with a brief assessment of our impact in the field.

Outline

1. How I got into patch antenna research
2. Basic geometry and basic characteristics of patch antennas
3. Our first topic
4. Our research on topics related to basic studies
5. Broadbanding techniques
6. Full wave analysis and CAD formulas
7. Dual/triple band designs
8. Designs for circular polarization
9. Reconfigurable patch antennas
10. Size reduction techniques
11. Concluding remarks and some citation data

Schedule

Part 1 (Hour 1)	Part 2 (Hour 2)	Part 3 (Hour 3)	Part 4 (Hour 4)
1. How I got into patch antenna research 2. Basic geometry and basic characteristics of patch antennas 3. Our first topic 4. Our research on topics related to basic studies	5. Broadbanding techniques 6. Full wave analysis and CAD formulas	7. Dual/triple band designs 8. Designs for circular polarization	9. Reconfigurable patch antennas 10. Size reduction techniques 11. Concluding remarks and some citation data

Main Reference

MICROSTRIP PATCH ANTENNAS

by

Kai Fong Lee *(The University of Mississippi, USA)*

Kwai Man Luk *(City University of Hong Kong, Hong Kong)*

About the Authors

Kai Fong Lee received his Ph.D. degree from Cornell University. He is Professor of Electrical Engineering at the University of Mississippi, where he served as Dean of Engineering from 2001 to 2009. He was the founding head of the Department of Electronic Engineering at City University of Hong Kong. An IEEE Fellow, he was the recipient of the 2009 John Kraus Antenna Award of the IEEE Antennas and Propagation Society for exceptional contributions to the field of antennas. He invented the wideband U-slot patch antenna and expanded the U-slot technique to small size, dual/triple band, and circular polarization applications.

Professor Kwai-Man Luk received the B.Sc.(Eng.) and Ph.D. from The University of Hong Kong. He is Director of the State Key Laboratory of Millimeter Waves at the City University of Hong Kong. He is the author of over 260 journal papers with over 2000 citations. He was awarded over 12 patents on the designs of various printed antennas. He is the Deputy Editor-in-Chief of the Journal of Electromagnetic Waves and Applications. He was a member of the Scientific Board, EC Network of Excellence in Antennas, Europe. Professor Luk is a Fellow of the Institute of Electrical and Electronics Engineers, Inc.

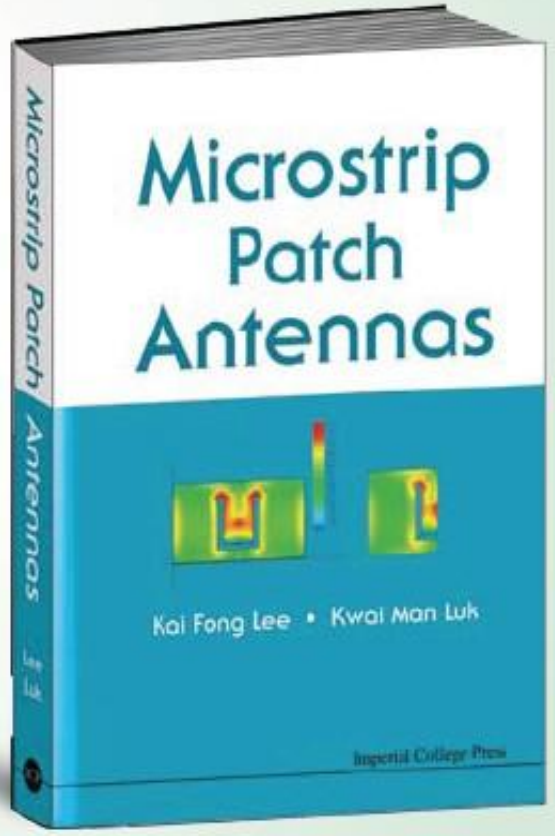

1. How I got into research on patch antennas

- **Research from 1965-1980: Theoretical plasma physics. 50 journal papers in physics journals**
- **First antenna papers: 1981; based on senior projects of CUHK students**
- **Attended 1981 IEEE AP meeting in Los Angeles; first exposed to papers on patch antenna research**
- **Had an idea on flight back to HK; teamed up with Dr. J. Dahele on patch antenna research.**
- **All subsequent papers (with many collaborators) were on patch antennas- no more on plasmas.**

1981 AP-S Meeting in Los Angeles: Two sessions on microstrip antennas

SESSION 1 MICROSTRIP ANTENNAS I
TUESDAY 8:30 - 12:00
SAN GABRIEL, Room C

Chairman: S. Long
University of Houston
Houston, TX

SESSION 12 MICROSTRIP ANTENNAS II
WEDNESDAY 1:30 - 5:00
SAN GABRIEL, Room A

Chairman: T. Itoh
University of Texas
Austin, TX

COLLABORATORS

Topic	Collaborators						
	CUHK	City Univ.	Univ. Akron	NASA	Univ. Toledo	Univ. Missouri	Univ. Mississippi
Basic Studies	Ho, Yeung, Wong, Dr. Dahele	Prof. Luk	Huynh				
Broadbanding		Tong, Mak, Guo, Prof. Luk	Huynh, Bobinchak	Dr. R. Lee			
Full wave analysis and CAD formulas					Chen, Fan		
Small-size wideband		Chair, Prof. Luk				Shackelford	Chair

(To be continued)

COLLABORATORS (continued)

Topic	Collaborators						
	CUHK	City Univ.	Univ. Akron	NASA	Univ. Toledo	Univ. Missouri	Univ. Mississippi
Circular Polarization		S.Yang, Prof. Luk					Khilde, Nayeri, S.Yang, Prof. Kishk, Profs. F. Yang & Elsherbeni
Dual/Triple Band		S.Yang, Mok, Wong, Prof. Luk					S. Yang, Prof. Kishk
Reconfigurable	Ho, Dr. Dahele	S.Yang					S. Yang, Khilde, Prof. Elsherbeni, Prof. F. Yang

2. Basic Geometry and Basic Characteristics of Patch Antennas

Patch antenna is a relatively new class of antennas developed over the last three and a half decades. The basic structure consists of an area of metallization supported above a ground plane and fed against the ground at an appropriate location.

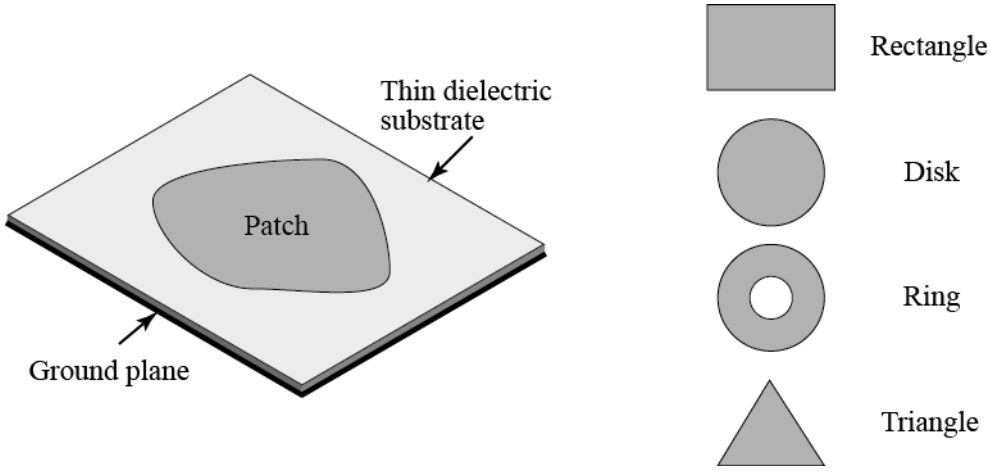

Fig. 1.1

2.1 Basic Geometries

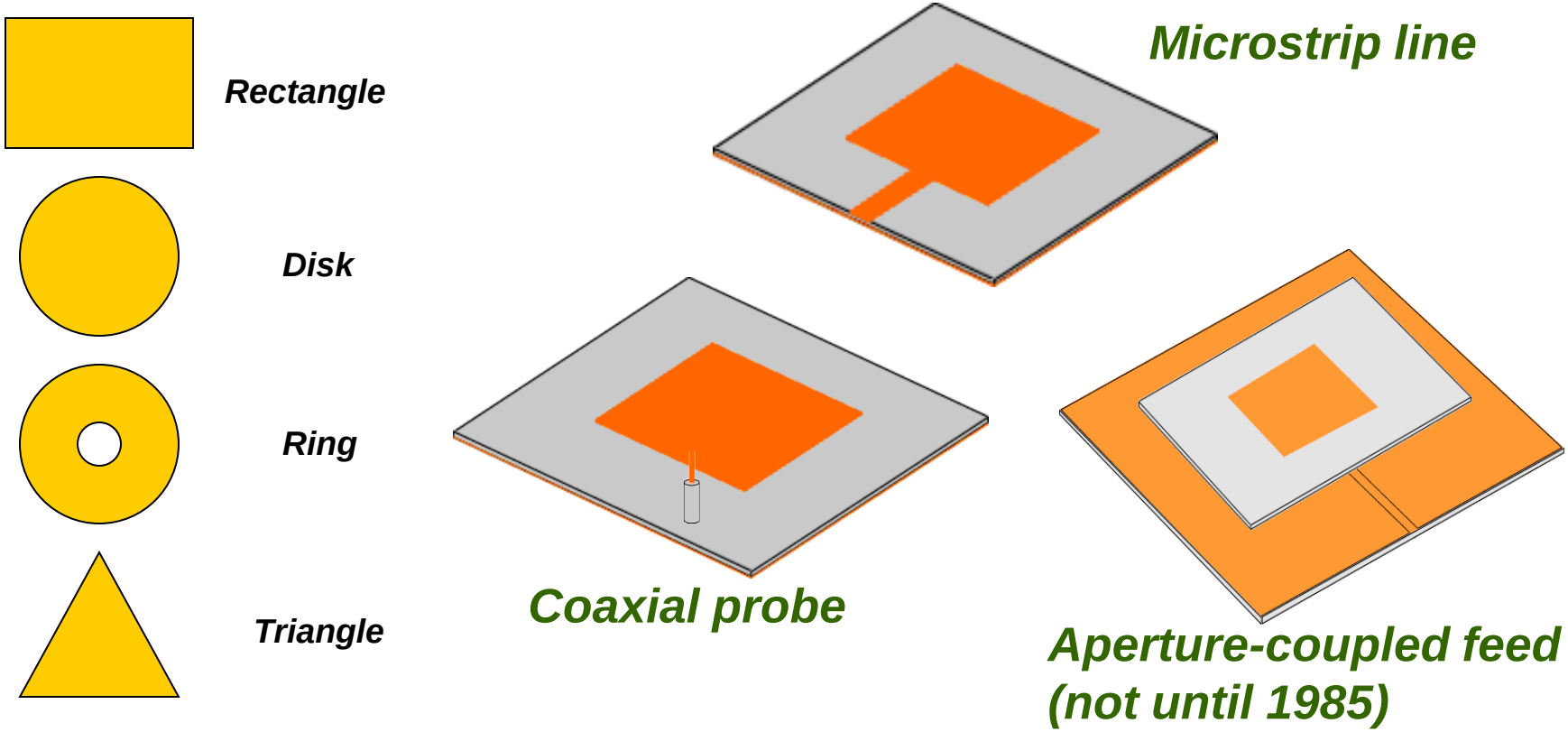

Patch geometry

Feeding methods

Fig. 1.2

2.2 Advantages and Disadvantages

2.2.1 Advantages

- Planar (can also be made conformal to shaped surface)
- Low profile
- Low radar cross-section
- Rugged
- Can be produced by printed circuit technology
- Can be integrated with circuit elements
- Can be designed to perform multiple functions.

2.2.1 Advantages

- These advantages make microstrip patch antennas much more suitable for aircraft, space craft, and missiles as they do not interfere with the aerodynamics of these moving vehicles.

Fig.1.3(a) Shuttle imaging radar antennas during flight

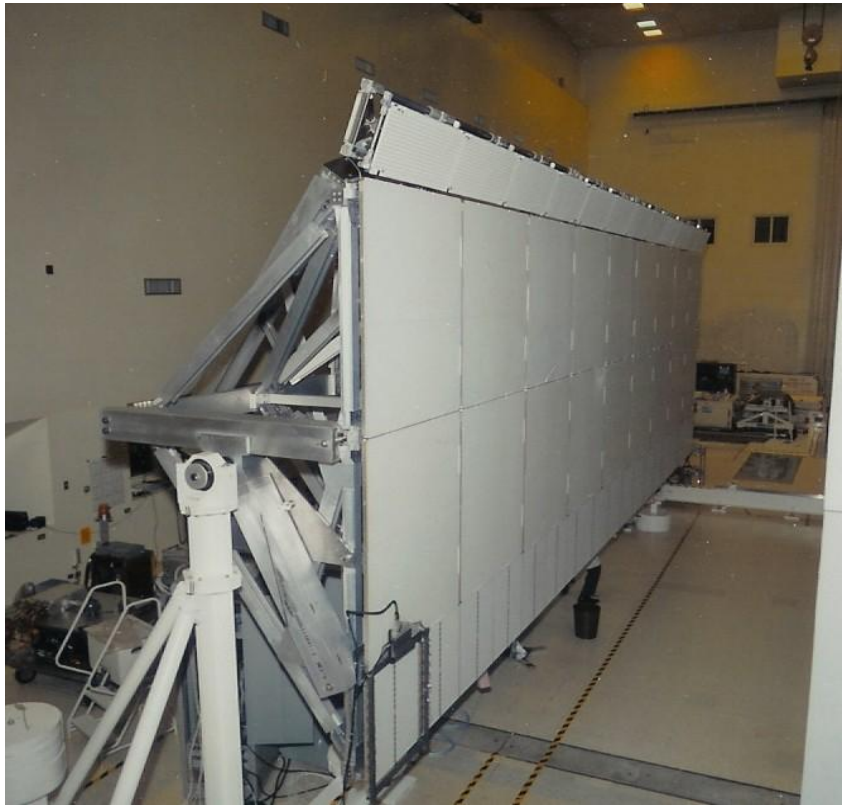

Fig. 1.3(b) Shuttle imaging radar antennas in laboratory

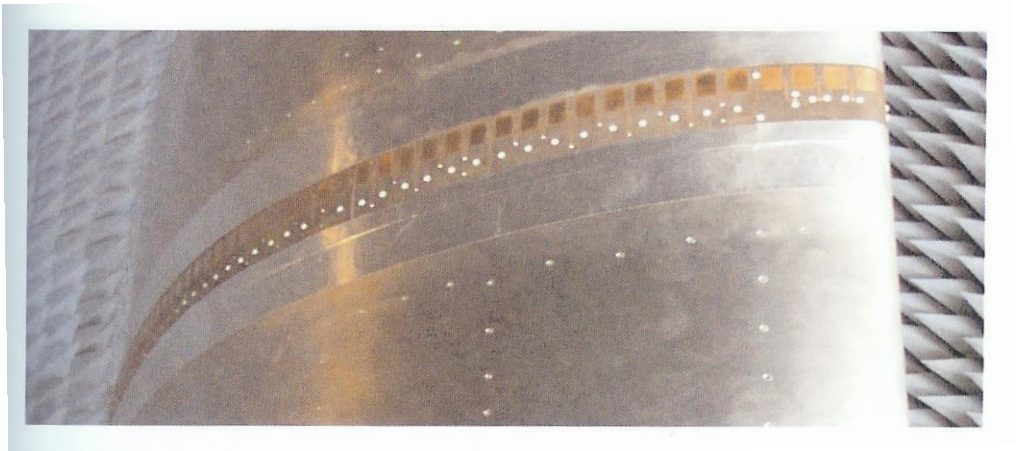

Fig.1.4 Conformal microstrip array on wing shape **Air Force Research Lab. Hanscom AFB, USA**

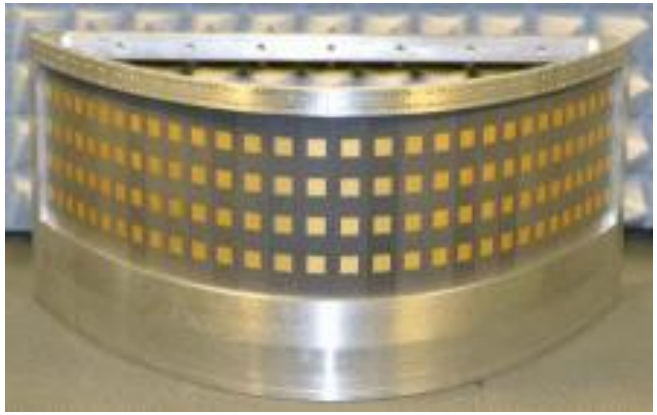

Fig. 1.5 Conformal Antenna Array **Fraunhofer Institute for High Frequency Physics and Radar Techniques**

2.2.1 Advantages

- These antennas have also become the favorites of antenna designers for commercial mobile and wireless communication systems.

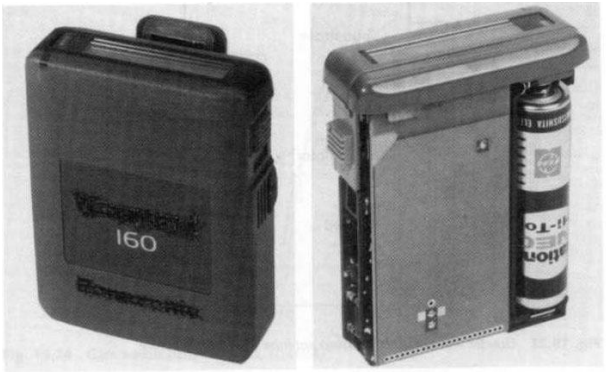

Antenna in Pager

Antenna in cellular phone

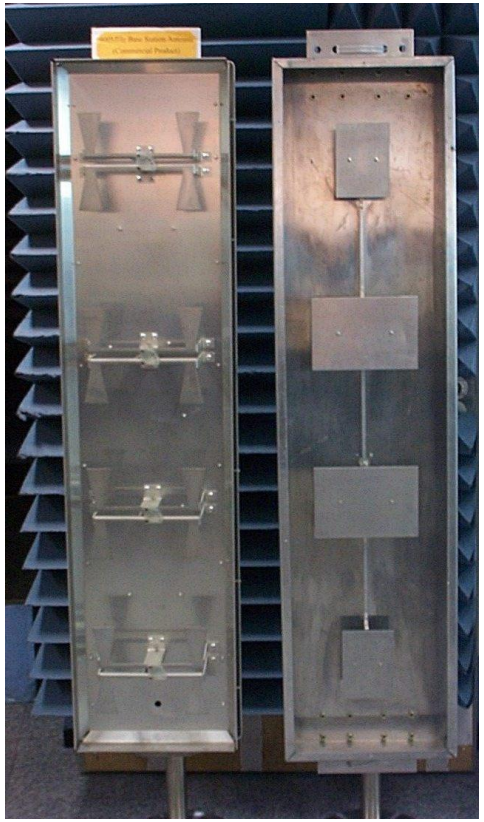

Base station antenna array

Fig. 1.6 Patch antennas in wireless communication systems

2.2 Advantages and Disadvantages

2.2.2 Disadvantages

- In its basic form, the microstrip antenna has a narrow bandwidth, typically less than 5 %. However, various bandwidth-widening techniques have been developed. Up to 50 % bandwidths have been achieved. It is generally true that wider bandwidth is achieved with the sacrifice of increased antenna physical volume.

- The microstrip antenna can handle relatively lower RF power due to the small separation between the radiating patch and its ground plane. Generally, a few tens watts of average power or less is considered safe.

2.2 Advantages and Disadvantages

2.2.2 Disadvantages

- While a single patch element generally incurs very little loss because it is only about one half wave long, microstrip arrays generally have larger ohmic loss than other types of antennas of equivalent aperture size. This ohmic loss mostly occurs in the dielectric substrate and the metal conductor of the microstrip line power dividing circuit.

2.3 Material Consideration

- Metallic patch is normally made of thin copper foil.
- Purpose of substrate material primarily to provide mechanical support for the radiating patch elements and to maintain the required spacing between the patch and its ground plane.
- The substrate thickness is in the range of 0.01 to 0.05 free-space wavelength.
- Dielectric constant range from 1 to 10. Can be separated into three categories:
  (1) Having a relative dielectric constant (relative permittivity) in the range of 1.0 to 2.0. This type of material can be air, Polystyrene Foam, or dielectric Honeycomb.
  (2) Having a relative dielectric constant in the range of 2.0 to 4.0 with material consisting mostly of Fiber-glass reinforced Teflon.

(3) With a relative dielectric constant between 4.0 and 10.0. The material can consist of Ceramic, Quartz, or Alumina.

- Most popular is Teflon-based with a relative permittivity between 2 and 3. The Teflon-based material, also named PTFE (PolyTeraFluoroEthylene), has a structure form very similar to fiberglass material used for digital circuit boards, but has a much lower loss tangent.

- For commercial application, cost is one of the most important criteria in determining the substrate. For example, a single patch or an array of a few elements may be fabricated on a low-cost fiberglass material at the L-band frequency, while a 20-element array at 30 GHz may have to use higher-cost, but lower loss, Teflon-based material (loss tangent less than 0.005).

- For a large number of array elements at lower microwave frequencies (below 15 GHz), a dielectric honeycomb or foam panel may be used as a substrate to minimize loss, antenna mass, and material cost while having increased bandwidth performance.

- There are materials with relative dielectric constant higher than 10. Patch size is smaller for higher dielectric constant. However, higher dielectric constant also reduces bandwidth and radiation efficiency.

2.4 Feed Methods for Single Element

2.4.1 Coax Probe Feed

- The coax probe is usually 50 Ω. The location of the probe should be at a 50 Ω point of the patch to achieve impedance matching
  - Type N, TNC, or BNC is for VHF, UHF, or lower microwave frequencies
  - OSM or OSSM can be used throughout microwave frequencies
  - OSSM, OS-50 or K-connector for millimeter-wave frequencies

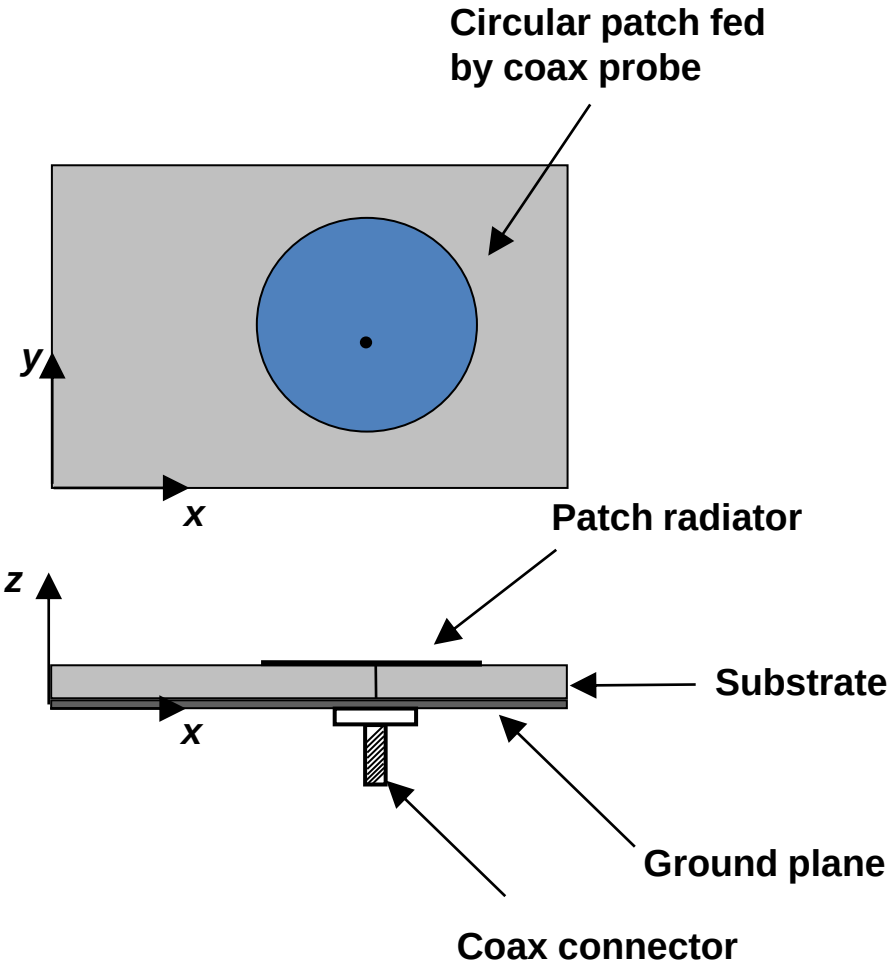

Fig. 1.7 Coaxial fed patch antenna

2.4 Feed Methods for Single Element

2.4.2 Microstrip-Line Feed

- A microstrip patch can be connected directly to a Microstrip transmission line.
- At the edge of a patch, impedance is generally much higher than 50 Ω (e.g. 200 Ω). To avoid impedance mismatch, sections of quarter-wavelength transformers can be used to transform a large input impedance to a 50 Ω line.

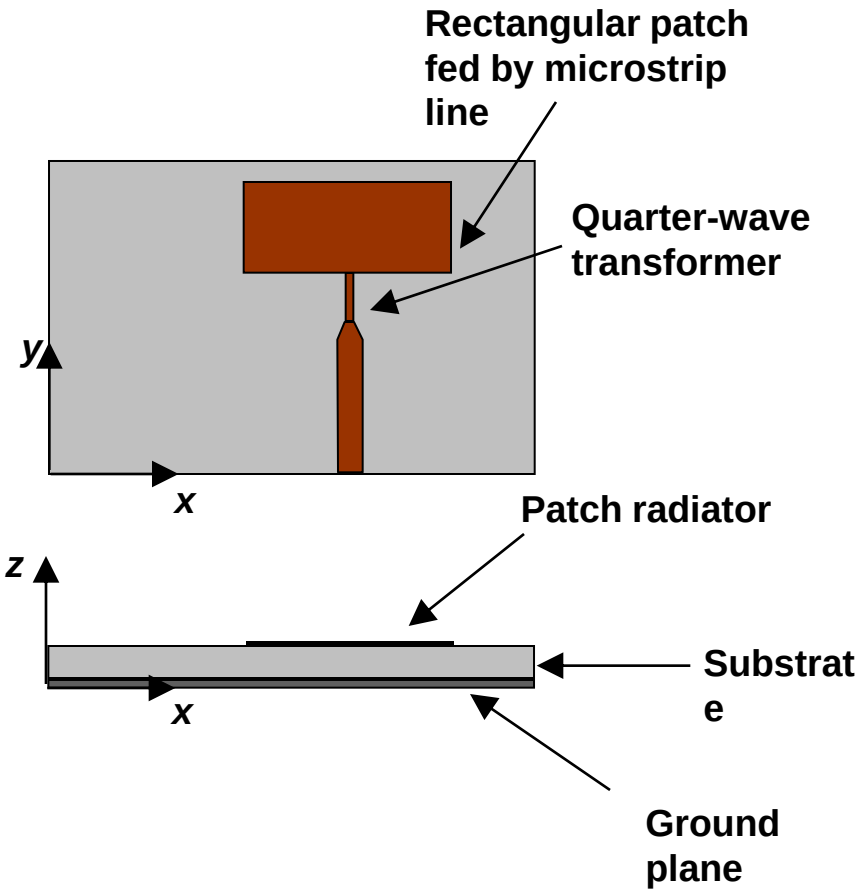

Fig. 1.8

2.4 Feed Methods for Single Element

2.4.2 Microstrip-Line Feed

- Another method of matching the antenna impedance is to extend the microstrip line into the patch, as shown.
- With this feed approach, array of patch elements and their microstrip power division lines can all be designed and chemically etched on the same substrate with relatively low fabrication cost per element. However, the leakage radiation of the transmission lines may be large enough to raise the sidelobe or cross-polarized levels of the array radiation.

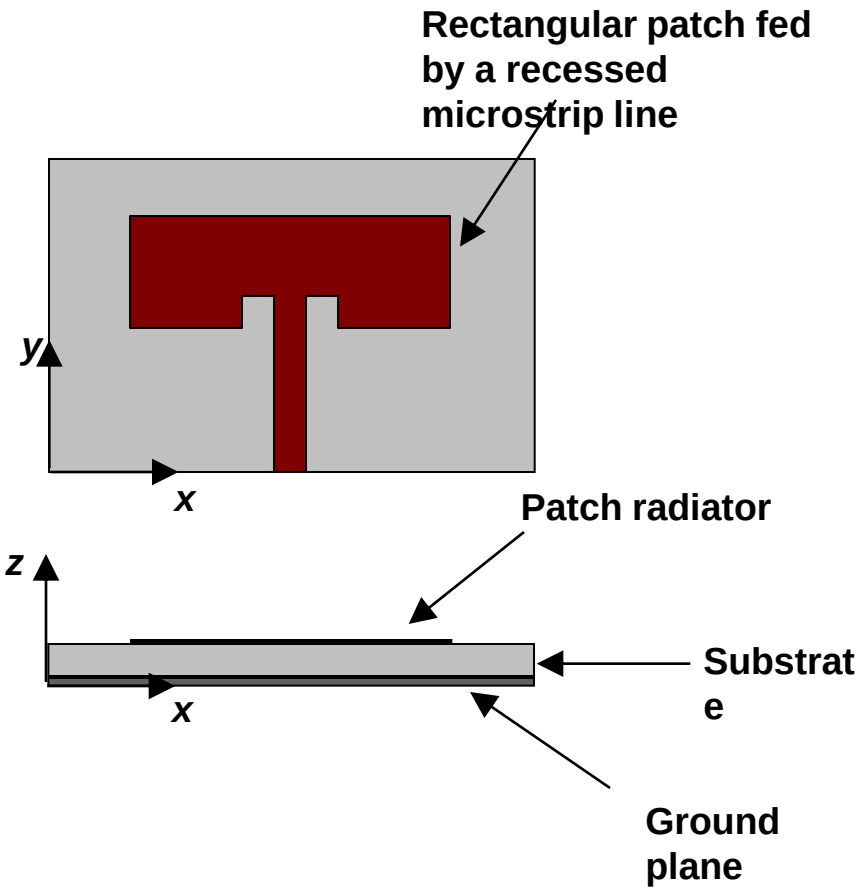

Fig. 1.9 Strip-line fed patch antenna

2.4 Feed Methods for Single Element

2.4.3 Aperture-Coupled Feed (D. M. Pozar 1985)

- An open-ended microstrip line can be placed on one side of the ground plane to excite a patch antenna suited on the other side through an opening slot in the ground plane. This slot-coupling or aperture-coupling technique can be used to avoid soldering connection as well as to avoid leakage radiation of the line to interfere with the patch radiation.

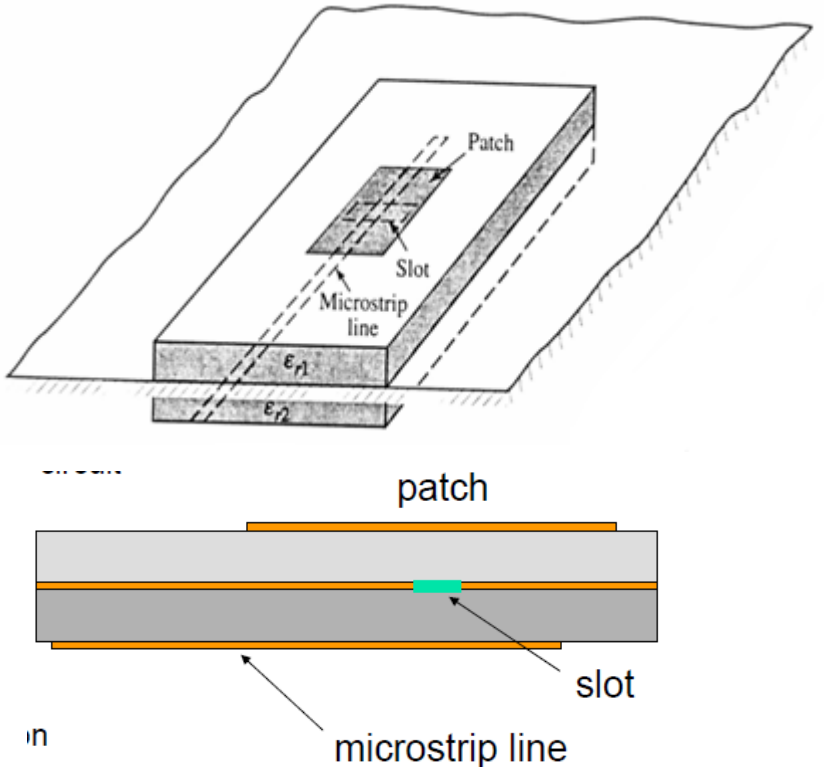

Fig. 1.10 Aperture-coupled fed patch antenna

2.4.3 Aperture-Coupled Feed

- In addition, this feed method allows the patch to achieve wide bandwidth (>10 %) with a thick substrate. The extra bandwidth that is achieved by this method when compared to the coax probe feed is generated by the coupling slot which is also a resonator and a radiator. When two resonators (slot and patch) having different but closely spaced resonance, wider bandwidth is achieved.
- A disadvantage is the back radiation from the slot.

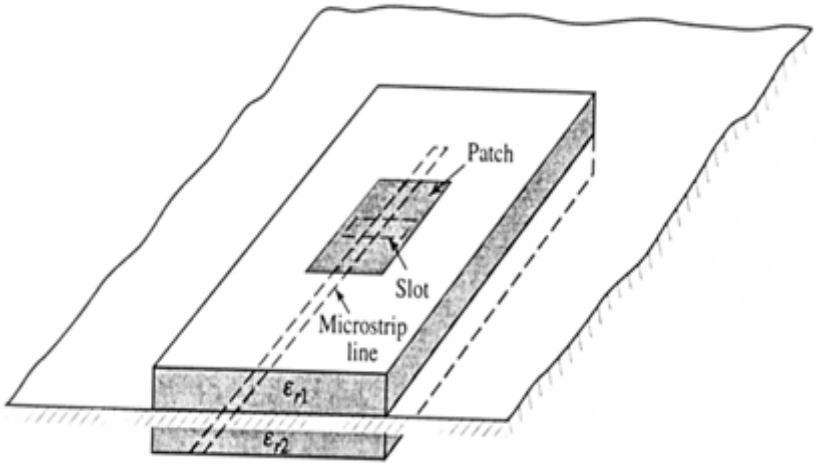

2.4.4 Summary of Advantages and Disadvantages of Feeding Methods

	Advantages	*Disadvantages*
Coaxial Feed	•Easy to match •Low spurious radiation	•Large inductance for thick substrate •Soldering required
Microstrip Line	•Monolithic •Easy to fabricate •Easy to match by controlling Insert position	•Spurious radiation from feed line, especially for thick substrate when line width is significant
Aperture Coupled	•Use of two substrates avoids deleterious effect of a high-dielectric constant substrate on the bandwidth and efficiency •No direct contact between feed and patch avoiding large probe reactance or wide microstrip line •No radiation from the feed and active devices since a ground plane separates them from the radiating patch	•Multilayer fabrication required •Higher backlobe radiation

2.5 The Cavity Model

The cavity model of the patch antenna was developed by Prof. Y. T. Lo of the University of Illinois and his associates and reported in two papers, one in 1979 (Lo et al.) and the other in 1981 (Richard et al.). It is a physical model based on a number of simplifying assumptions. It is used extensively before commercial simulation softwares were available, especially for coaxially fed patch antennas.

Prof. Y. T. Lo of the University of Illinois, Urbana Champaign

We briefly summarize the essential features below.

2.5.1 The Leady Cavity

Consider first the region between the patch and the ground plane.

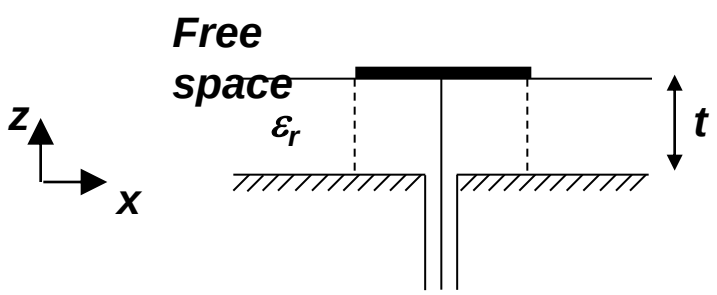

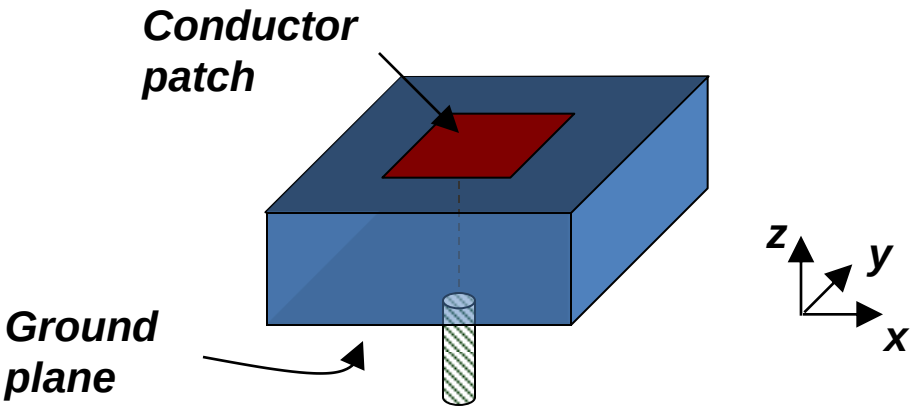

This resembles an electromagnetic resonator or cavity, excited by a coaxial probe. In the usual cavity, the vertical walls are also conducting walls

The fields inside the conducting box are obtained by solving Maxwell's equations in the region inside the box and demanding its solutions to satisfy the boundary conditions of $\boldsymbol{E}_t = 0$ on the top, bottom, and on its sides.

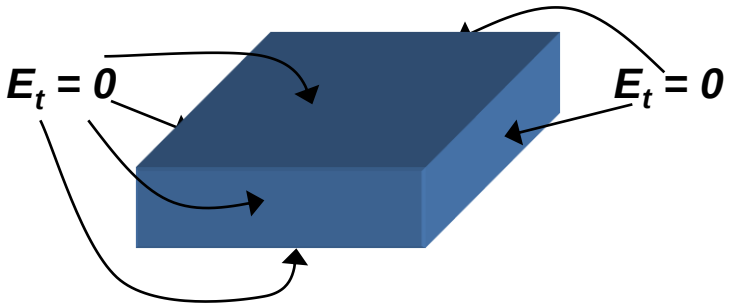

This leads to the discrete set of characteristic frequencies or resonant frequencies and discrete set of field patterns or modes.

- In The patch antenna case, the side walls are not enclosed by conducting walls and the fields inside the cavity can leak out to space, leading to radiation and an antenna results. Since the radiation fields can be calculated from the fields at the exit region, we first need to find the fields in the cavity. To do this, we need to know what boundary condition to impose on the side (vertical) walls.
- It turns out that if the substrate is thin so that $t \ll \lambda$ where λ is wavelength, the boundary condition is $H_t = 0$ on the side walls and the boundary value problem to solve is

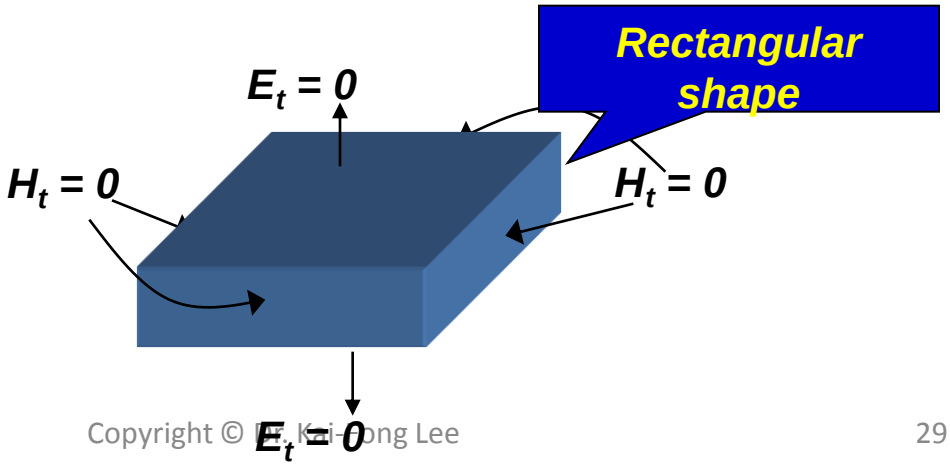

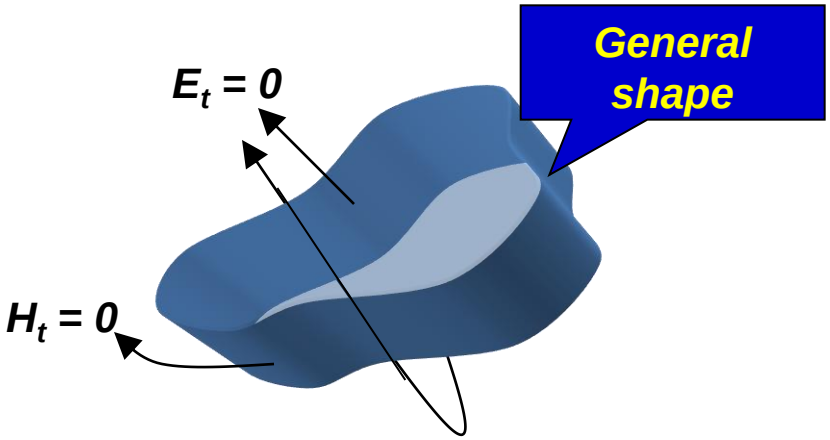

2.6 Basic characteristics

In the late 1970's and 1980's, the cavity model was used to predict the basic characteristics of the probe-fed rectangular, circular, annular-ring and equitriangular patch antennas, and the results were verified experimentally. While differing in detail, there are a number of similar features, irrespective of the shapes of the patch. To be specific, the essential features are delineated below for the coaxially fed (also known as probe fed) rectangular patch shown in Fig. 11.

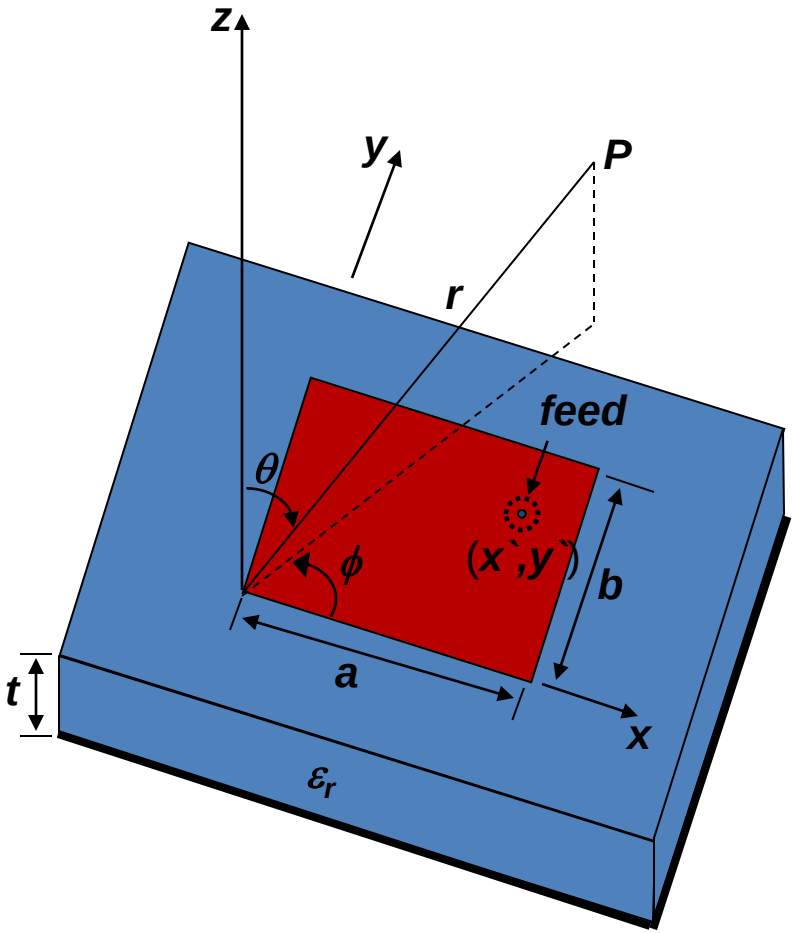

Fig. 1.11 Geometry of the coaxially fed rectangular patch antenna

A. **The fields under the cavity are transverse magnetic, with the electric field in the z direction and independent of z. There are an infinite number of modes, each characterized by a pair of integers (m, n):**

$$E_z = E_0 \cos\frac{m\pi x}{a}\cos\frac{n\pi y}{b}$$

B. For the cavity bounded by electric walls ($E_t = 0$) on the top and a magnetic wall ($H_t = 0$) on the side, the resonant frequency of each mode is governed by the dimensions of the patch and the relative permittivity of the substrate ε_r. It is given by

$$k_{mn}^2 = \left(\frac{m\pi}{a}\right)^2 + \left(\frac{n\pi}{b}\right)^2$$

$$f_{mn} = k_{mn} c / 2\pi\sqrt{\varepsilon_r}$$

Example

$$k_{10} = \frac{\pi}{a}$$

$$f_{10} = \frac{c}{2a\sqrt{\varepsilon_r}} \quad \Rightarrow \quad a = \frac{c}{2 f_{10}\sqrt{\varepsilon_r}}$$

$$\text{If} \quad f_{10} = 1GHz \quad , \ \varepsilon_r = 2.1$$

$$a = 10.34\,cm$$

C. **Because of fringing fields at the edge of the patch, the patch behaves as if it has a slightly larger dimension. Semi-empirical correction factors are usually introduced in the cavity-model-based design formulas to account for this effect, as well as the fact that the dielectric above the patch (usually air) is different from the dielectric under the patch. These factors vary from patch to patch.**

For the rectangular patch, with a > b, a commonly used formula for the fundamental mode, accurate to within 3% of measured values, is

$$f_r = \frac{c}{2(a+t)\sqrt{\varepsilon_e}}$$

where

$$\varepsilon_e = \frac{(\varepsilon_r + 1)}{2} + \frac{(\varepsilon_r - 1)}{2}\left[1 + \frac{10t}{b}\right]^{\frac{-1}{2}}$$

is the effective permittivity.

D. **The equivalent sources at the exit region (the vertical side walls) are the surface magnetic current densities, related to the tangential electric fields in those locations. The tangential electric field (or magnetic surface current distributions) on the side walls for the lowest two modes, TM_{01} and TM_{10} , are illustrated in Fig. 12. For the TM_{10} mode, the magnetic currents along b are constant and in phase while those along a vary sinusoidally and are out of phase. For this reason, the "b" edge is known as the radiating edge since it contributes predominantly to the radiation. The "a" edge is known as the non-radiating edge. Similarly, for the TM_{01} mode, the magnetic currents are constant and in phase along a and are out of phase and vary sinusoidally along b. The "a" edge is thus the radiating edge for the TM_{01} mode.**

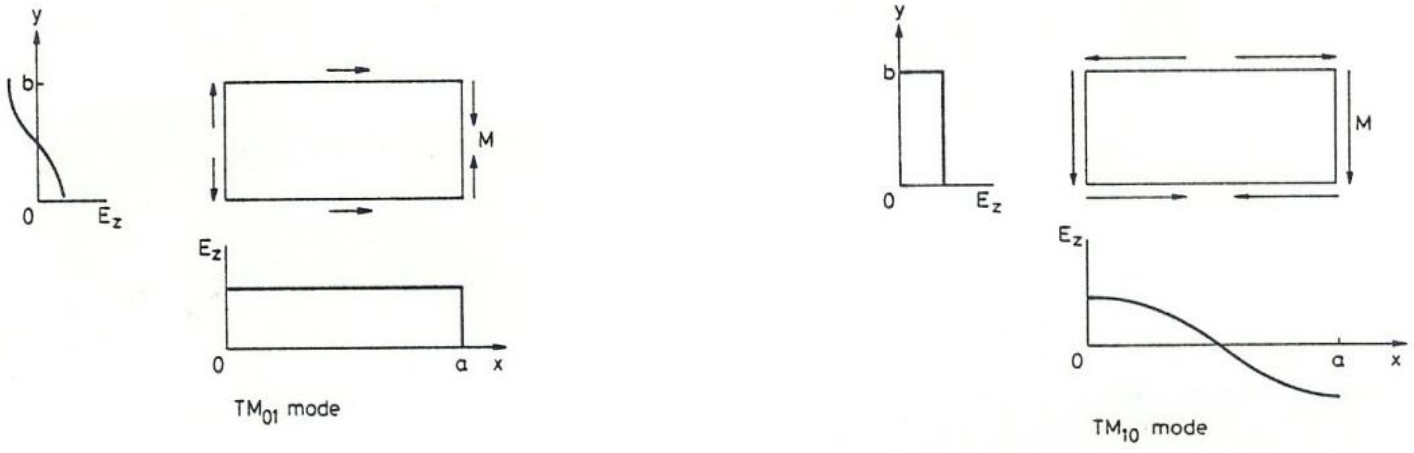

Fig.1.12 Tangential electric field on the side walls of the cavity under the rectangular patch.

E. To satisfy the boundary condition imposed by the feed, the fields under the patch are expressed as a summation of the various modes. The mode with resonant frequency equal to the excitation frequency will be at resonance and has the largest amplitude. Its polarization is called co-polarization. If the off-resonant modes have polarizations orthogonal to the polarization of the resonant mode, they contribute to the cross-polarization.

F. Each resonant mode has its own characteristic radiation pattern. For the rectangular patch, the commonly used modes are TM_{10} or TM_{01}. However, the TM_{03} mode has also received some attention. These three modes all have broadside radiation patterns. The computed patterns for a=1.5b and two values of ε_r are shown in Fig. 1.13. In the principal planes, the TM_{01} and TM_{03} modes have similar linear polarization while that of the TM_{10} mode is orthogonal to the other two. The patterns do not appear to be sensitive to a/b or t. However, they change appreciably with ε_r. Typical half-power beamwidths of the TM_{10} and TM_{01} modes are of the order of 100^0 and the gains are typically 5 dBi. The patterns of most of the other modes have maxima off broadside. For example, those of the TM_{11} mode are illustrated in Fig. 13(g) for ε_r =2.32.

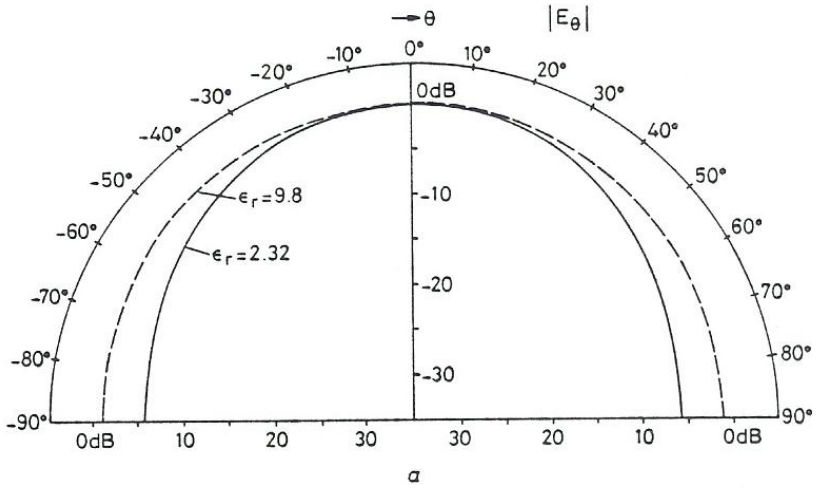

a

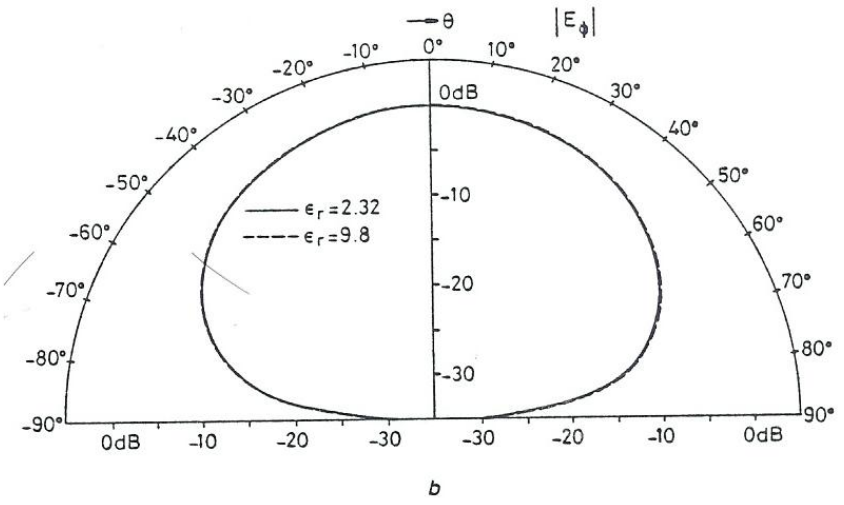

b

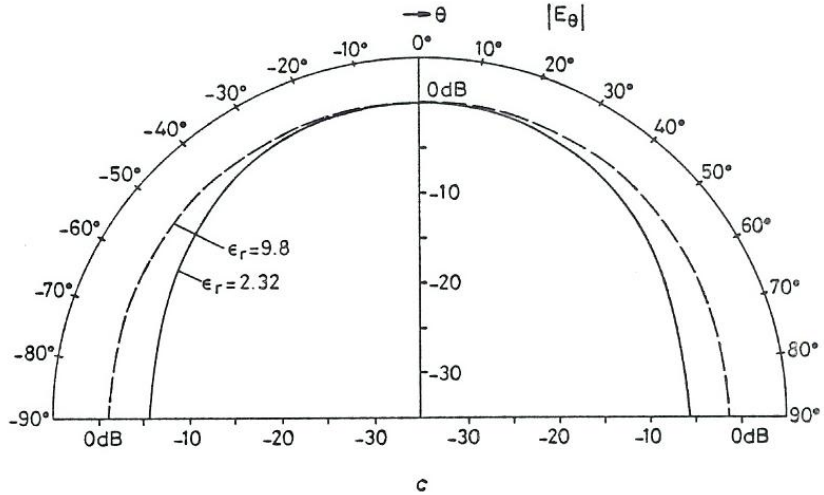

c

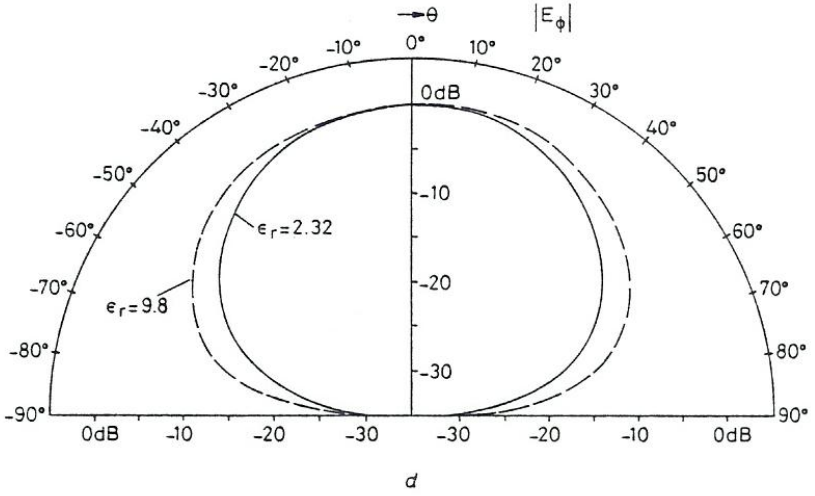

d

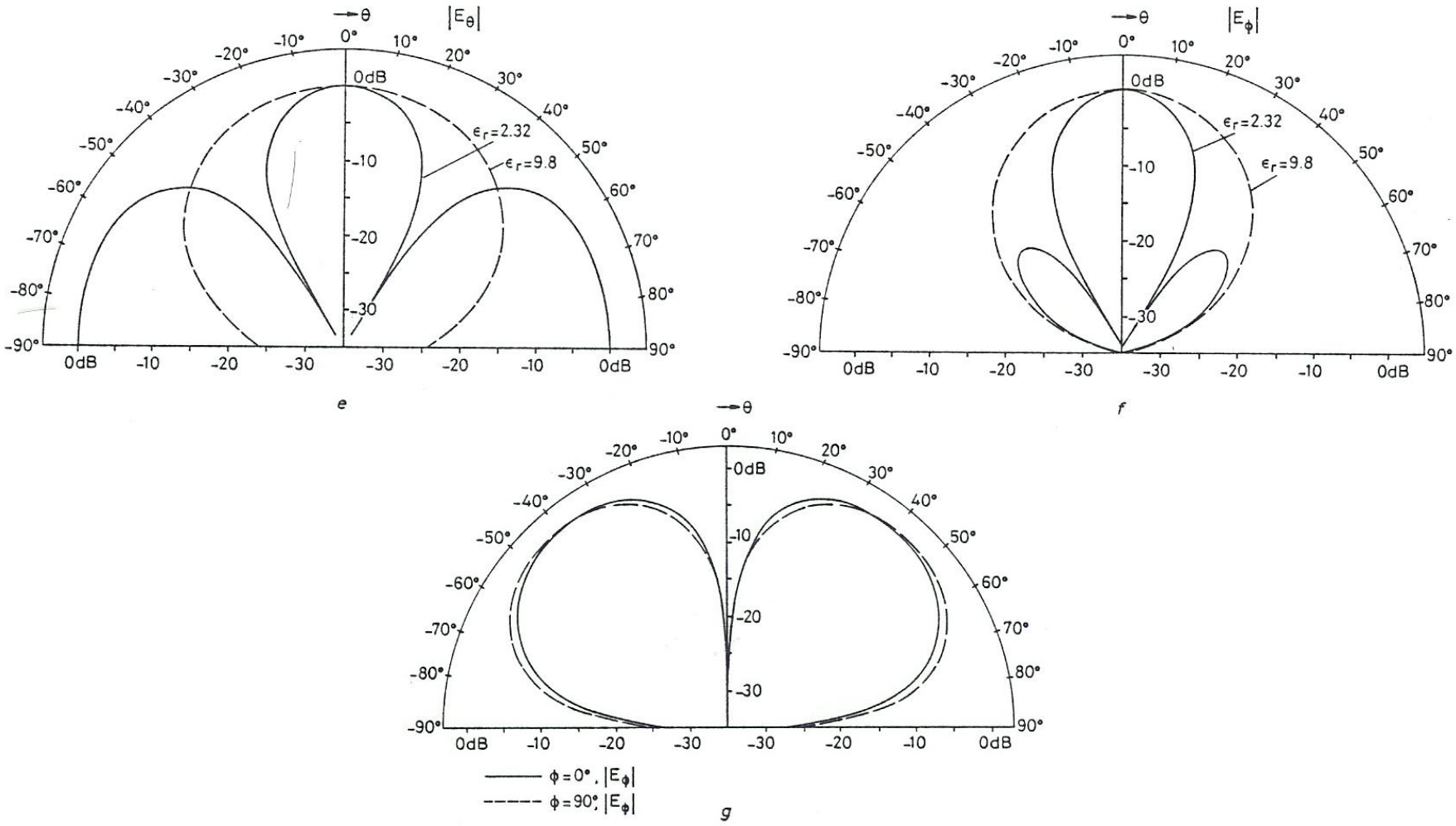

Fig. 1.13 Relative field patterns for a rectangular patch with a/b=1.5, f_{nm} = 1 GHz, and (i) ε_r = 2.32, t=0.318, 0.159, 0.0795 cm; (ii) ε_r = 9.8, t=0.127, 0.0635, 0.0254 cm. (a) TM_{10}, ϕ = 0°. (b) TM_{10}, ϕ = 90°. (c) TM_{01}, ϕ=90° . (d) TM_{01}, ϕ = 0°.(e) TM_{03}, ϕ = 90°. (f) TM_{03}, ϕ = 0°. (g) TM_{11}, ε_r = 2.32.

For each mode, there are two orthogonal planes in the far field region – one designed as E-plane and the other designed as H-plane. The patterns in these planes are referred to as the E and H plane patterns respectively. One can show from the equations obtained from the cavity model that for the TM_{01} mode, the y-z plane ($\phi = 90^0$) is the E-plane and the x-z plane ($\phi = 0^0$) is the H plane. For the TM_{10} mode, the x-z plane is the E-plane and the y-z plane is the H plane.

With appropriate design, circular polarization can be achieved by utilizing the two modes. This will be discussed later.

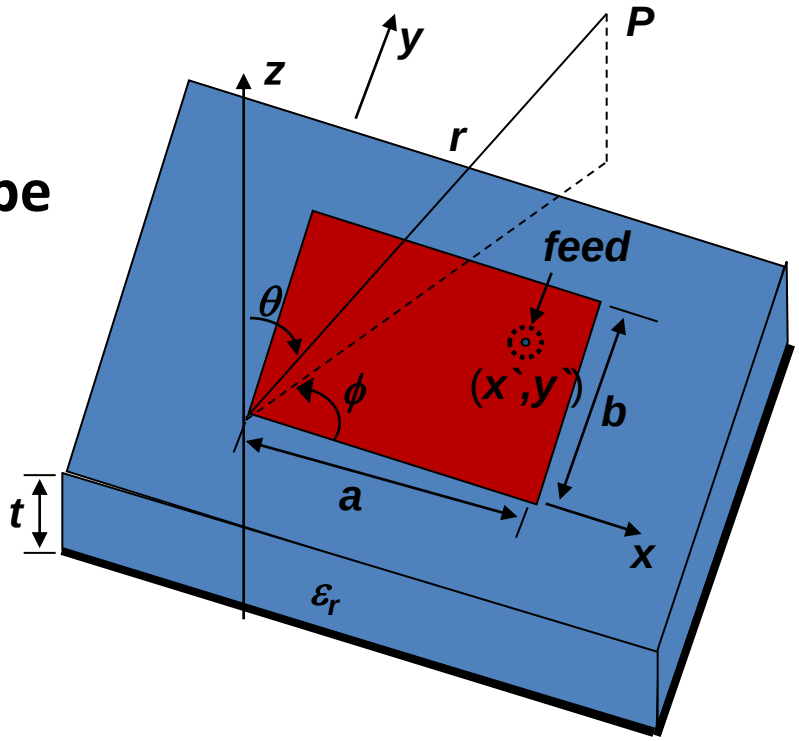

G. **At resonance, the input reactance is small for thin substrates while the input resistance is largest when the feed is near the edge of the patch and decreases as the feed moves inside the edge. The decrease follows the square of a cosine function for the TM_{10} and TM_{01} modes of a coaxial feed rectangular patch. Fig.1.14 shows the theoretical and measured values of the resonant resistance of the first two mode of a coaxial fed rectangular patch.**

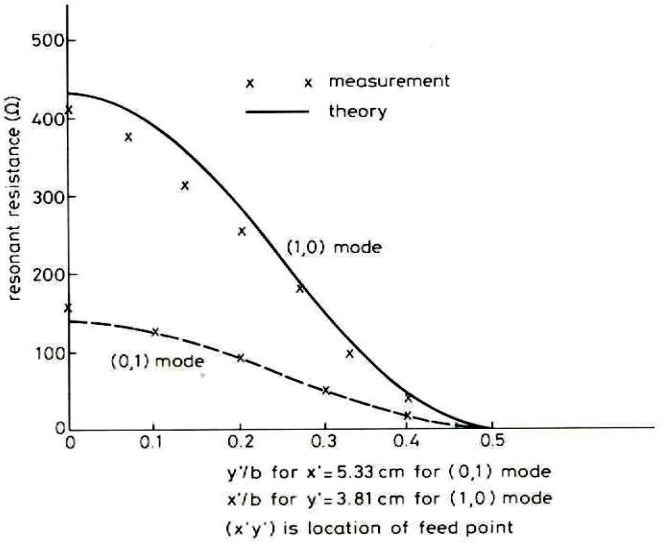

Fig. 1.14 From Lo et al. 1981.

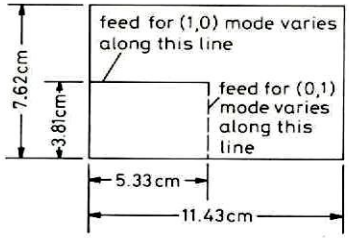

rectangular microstrip antenna using 1/16" rexolite 2200

H. By choosing the feed location properly, the resonant resistance can be matched to the feedline resistance, while the use of thin substrates (thickness $t < 0.03 \lambda_0$) will minimize the feed inductance at resonance, resulting in a voltage standing wave ratio (VSWR or SWR) very near unity. As the frequency deviates from resonance, VSWR increases. For linear polarization, a common definition of impedance bandwidth is the range of frequencies for which VSWR is less than or equal to two, corresponding to 10 db return loss or -10 dB for the reflection coefficient S_{11} . This is usually also the antenna bandwidth, as the patterns are much less sensitive to frequency. For circular polarization, bandwidth is determined by both VSWR < 2 and axial ratio < 3 dB.

I. The losses in the patch antenna comprises radiation, copper, dielectric, and surface wave losses. For thin substrates, surface wave can be neglected. It was found, if the antenna is to launch no more than 25% of the total radiated power as surface waves, the requirement is $t/\lambda_0 < 0.07$ for $\varepsilon_r = 2.3$ and $t/\lambda_0 < 0.023$ for $\varepsilon_r = 9.8$. The quality factor Q of a particular mode is determined by the ratio of the stored to loss energy and determines the impedance bandwidth of the antenna. The larger the losses, the smaller the Q and the larger the bandwidth.

J. In general, the impedance bandwidth is found to increase with substrate thickness t and inversely proportional to ε_r. However, use of low permittivity substrates can lead to high levels of radiation from the feed lines while for higher permittivities, an increase in substrate thickness can lead to decrease in efficiency due to surface wave generation. Additionally, when the substrate thickness exceeds about $0.05\,\lambda_0$, where λ_0 is free space wavelength, the antenna cannot be matched to the feedline due to the inductance of the feed. As a result, for the basic MPA geometry, the impedance bandwidth is limited to about 5%.

2.7 Limitations of the Cavity Model Analysis

The basic assumption which renders the calculations of the cavity model relatively simple is that the substrate thickness is assumed to be much smaller than wavelength so that the electric field has only a vertical (z) component which does not vary with z. From this it follows that:

(1) The fields in the cavity are TM (transverse magnetic).

(2) The cavity is bounded by magnetic walls ($H_t = 0$) on the sides.

(3) Surface wave excitation is negligible.

(4) The current in the coaxial probe is independent of z.

The coaxial probe is modeled by a current ribbon of a certain width, which is a free parameter chosen to fit the experimental data.

There are a number of limitations to the cavity model even if the thin substrate condition is satisfied. The magnetic wall boundary condition leads to resonant frequencies which do not agree well with experimental observations, and an ad hoc correction factor has to be introduced to account for the effect of fringing fields. The width of the current ribbon used to model the coaxial probe is another ad hoc parameter. The model cannot handle designs involving parasitic elements, either on the same layer or on another layer. It cannot analyze microstrip antennas with dielectric covers. When the thickness of the substrate exceeds about 2% of the free space wavelength, the cavity model results begin to become inaccurate, due to the breakdown of (1)-(4).

Despite the limitations described above, the cavity model has the advantage of being simple and providing physical insight. In the early 1980's, it was used to obtain the basic characteristics and design information for rectangular, circular, annular, and triangular patches and compared with measurements.

REFERENCES

- Y. T. Lo, D. Solomon, and W. F. Richards, "Theory and experiment on microstrip antennas," *IEEE Trans. Antennas Propagat*., Vol. AP-27, pp. 137-145, 1979.

- W. F. Richards, Y. T. Lo and D. D. Harrison, "An improved theory for microstrip antennas and applications," *IEEE Trans. Antennas Propagat*., Vol. AP-29, pp. 38-46, 1981.

- K. F. Lee and J. S. Dahele, "Characteristics of microstrip patch antennas and some methods of improving frequency agility and bandwidth," in Handbook of Microstrip Antennas, J. R. James and P. S. Hall (Editors), Peter Peregrinus, Ltd., London, 1989.

- C. Wood, "Analysis of microstrip circular patch antennas," *IEE Proc*. Vol. 128H, pp. 69-76, 1981.

2.8 Full Wave Analysis

Another approach to find the characteristics of microstrip patch antennas is via full wave analysis, which involves solving Maxwell's equations subject to the boundary conditions (Integral equations approach; finite difference time domain; finite element). In the early 1980's, the main attention was in the integral equation approach, led by D. M. Pozar and J. R. Mosig. The following is one way of describing the procedure of the integral equation approach.

***Procedure for Integral Equation Approach*:**

- Write down the solutions to the wave equation in the transformed domain for the different regions of the structure (substrate, air). The solutions contain arbitrary coefficients.
- The boundary conditions across the interfaces, at infinity and on the ground plane are used to obtain the coefficients of the fields. The surface current densities on the patch are regarded as unknowns while the current on the feed is regarded as given.
- The condition that the tangential electric fields vanish on the patch leads to integral equations for the surface currents.
- The surface current densities and the resonant frequencies are solved by a numerical technique known as the Method of Moments.
- Once the surface current densities are obtained, various characteristics such as input impedance and the radiation patterns can be computed.

D. M. Pozar

Advantages of the Full-wave Method

- No-AD HOC correction factor
- In principle good for thick substrate
- Can handle dielectric cover and parasitic elements
- Can handle arbitrary patch shape

J. R. Mosig

Disadvantages of the Full-wave Method

- Need extensive computation time
- Little physical insight

In the early 1980's, use of full-wave method was not widespread. Commercial simulation softwares based on full-wave method were not yet available.

2.9 State of patch antenna in the early 1980's

The state of patch antenna in the early 1980's can be partially summarized below:

A. The characteristics of rectangular and circular patches were largely established theoretically (via cavity model) and verified experimentally. However, information on cross polarization characteristics was sketchy.

B. Partial information was obtained for the annular-ring patch and the equitriangular patch.

C. Narrow bandwidth was widely recognized as a problem and interest in frequency tuning and broadbanding techniques began to appear.

D. Full wave methods were being developed.

3. Our first topic - Patch antenna with air gap

3.1. Introduction

In many applications, it is necessary for the antenna to receive several adjacent frequencies (e.g. channels). The patch antenna in its basic form is inherently narrow band and may not have the necessary bandwidth. Methods of tuning the operating frequency of the patch antenna are therefore of interest. In 1981 (the time I attended the AP meeting in Los Angeles), there were two methods proposed: (1) using varactor diodes; (2) using shorting posts.

3.2 Varactor Diodes – Electronic Tuning

- **For a given set of patch dimensions, the resonant frequency is primarily governed by the value of the relative permittivity ε_r of the substrate. If some means is available to alter ε_r , the resonant frequency will change. One method of achieving this is to introduce varactor diodes between the patch and the ground plane, as shown in Fig. 1.15.**
- **The diodes are provided with a bias voltage, which controls the varactor capacitance and hence the effective permittivity of the substrate. Bhartia and Bahl [1982] performed an experiment on this method and the results are shown in Fig. 1.16.**
- **The resonant frequency of the lowest mode increases with the bias voltage. A tuning range of some 20 % was achieved with a 10 V bias. The range increased to about 30 % with a 30 V bias. The relationship is not linear.**

3.2 Varactor Diodes – Electronic Tuning

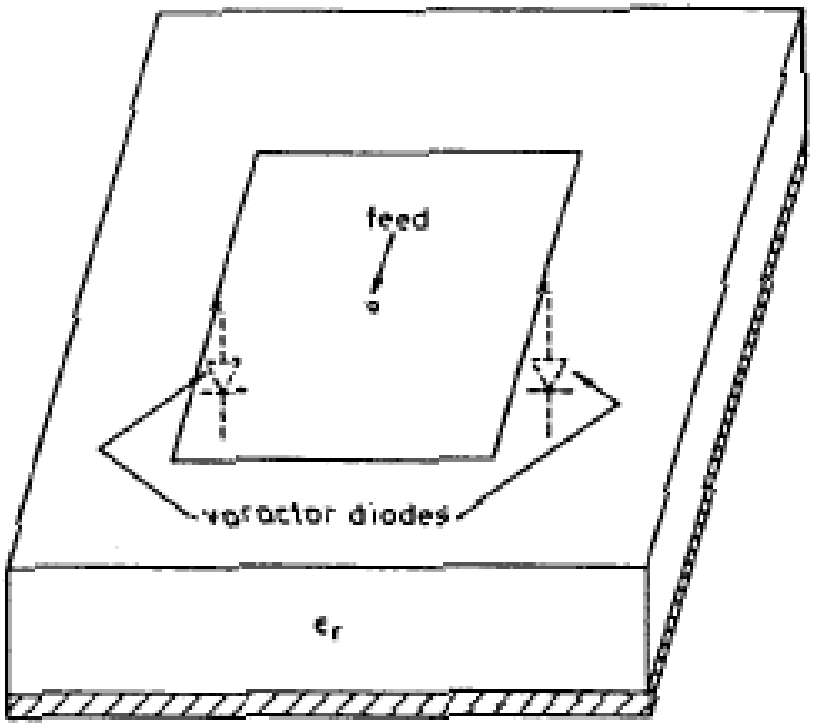

Fig. 1.15. Illustrating the use of varactor diodes for tuning.

3.2 Varactor Diodes – Electronic Tuning

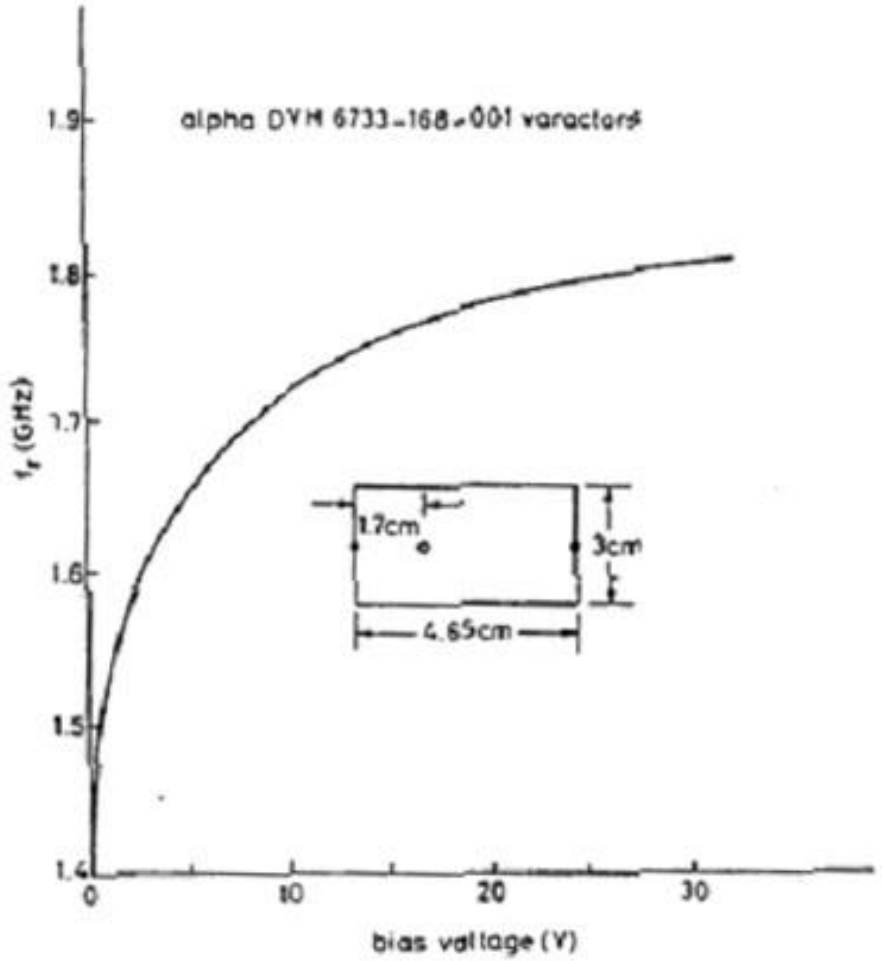

Fig. 1.16. Resonant frequency versus bias voltage for a varctor-loaded rectangular patch antenna.

3.3. Tuning Using Shorting Posts (Pins)

- **The value of ε_r can also be changed by introducing shorting posts (pins) at various points between the patch and the ground plane. These shorting posts present an inductance, and therefore affect the effective permittivity of the substrate. The method appeared to be first introduced by Schaubert et al. in 1981, who performed an experiment on a rectangular patch using two pins, as shown in Fig. 1.17.**

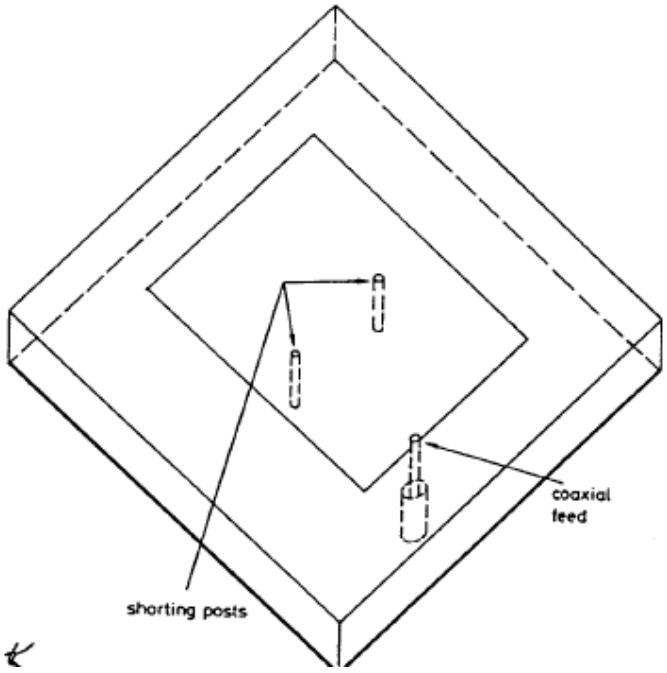

Fig. 1.17. Illustrate the use of shorting posts for tuning the resonant frequency of a patch antenna.

3.3 Tuning Using Shorting Posts (Pins)

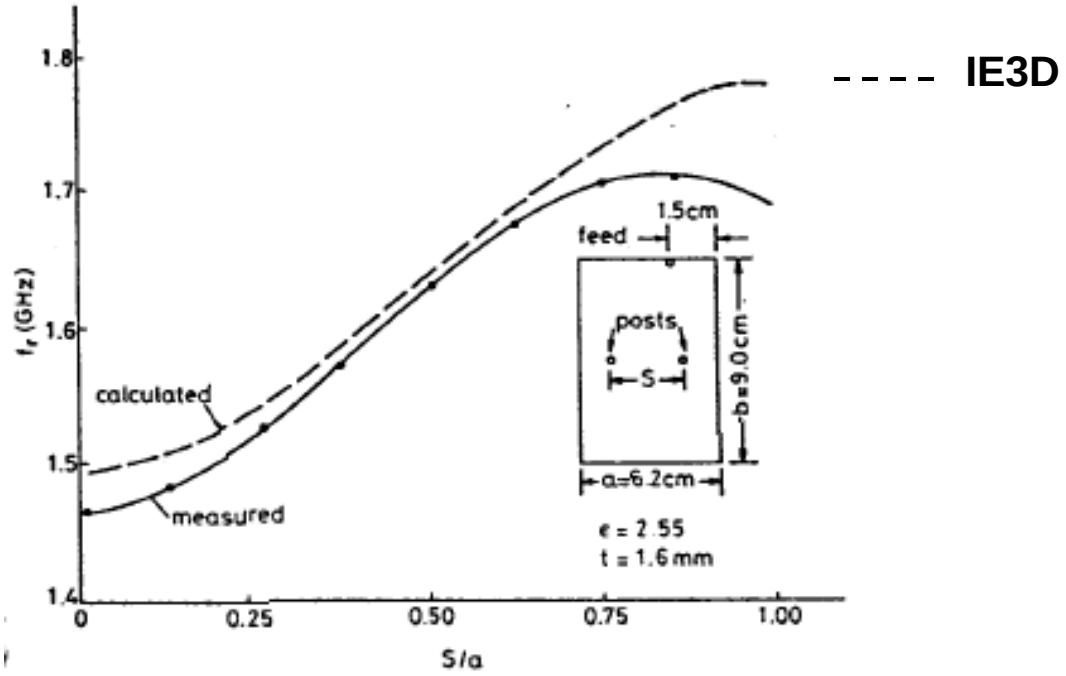

Fig. 1.18 Resonant frequency versus separation of posts for 6.2 × 9.0 cm rectangular patch antenna with ε_r = 2.55, t = 1.6 mm.

- The solid curve in Fig.1.18 shows that the resonant frequency is dependent on the separation of the two posts. A tuning range of some 18 % is obtained as the separation varies between 0 and the whole width of the patch.

3.4 Tuning by Means of an Adjustable Air-gap

3.4.1 Geometry of a Microstrip Patch Antenna with Air-Gap

- On the flight back from the AP meeting in Los Angeles in 1981, I came up with the air gap idea to tune the frequency of a patch antenna. The geometry of a microstrip patch antenna with an air gap is shown in Fig. 18.

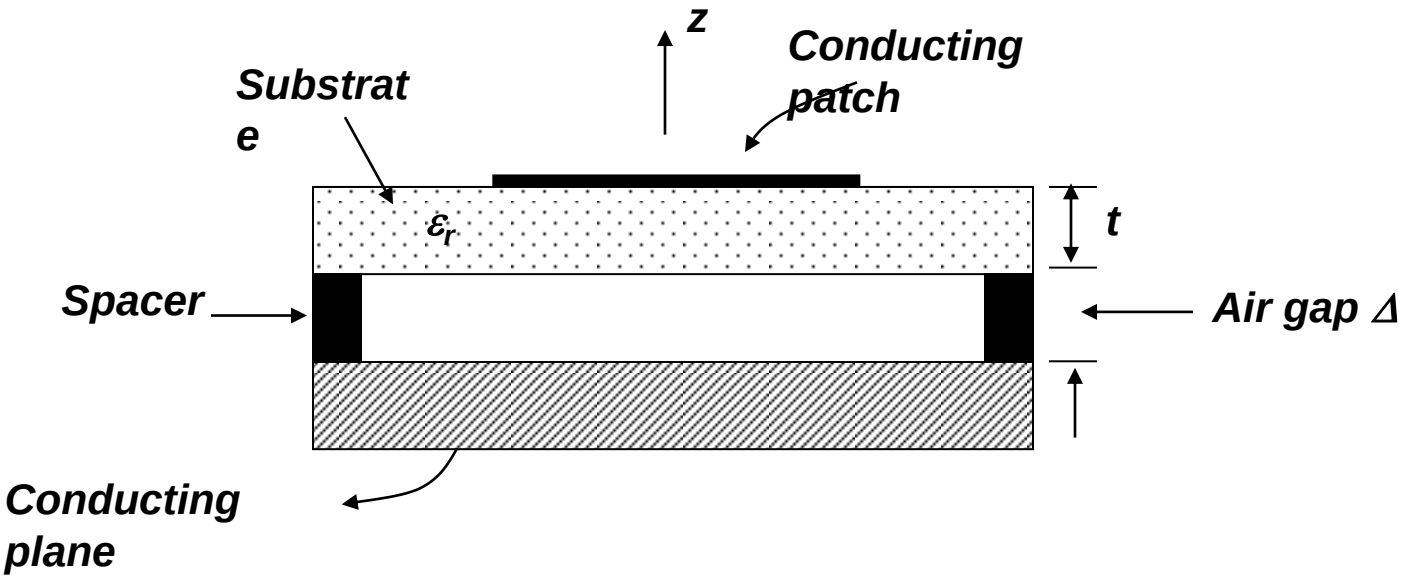

Fig. 1.19 Geometry of a microstrip patch antenna with an air gap

3.4 Tuning by Means of an Adjustable Air-gap

3.4.1 Geometry of a Microstrip Patch Antenna with Air-Gap

- The air gap lowers the effective permittivity of the cavity under the patch. Hence the resonant frequencies of the various modes will increase.
- The resonant frequencies can be tuned by adjusting the air gap width Δ.
- Substrate and etching tolerances can be compensated by adjusting Δ.
- Bandwidth will increase, partly due to the increase in the height of the dielectric medium and partly because the effective permittivity is now lower.
- Can be applied to patches of arbitrary shape.

3.4 Tuning by Means of an Adjustable Air-gap

3.4.2 Effective Permittivity – Heuristic Derivation

- Consider the capacitance of a capacitor with two dielectric layers,

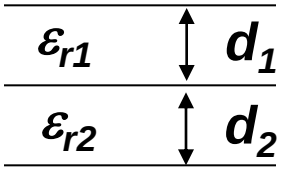

Fig. 1.20

$$C_1 = \varepsilon_1 A / d_1 \qquad A = area$$

$$C_2 = \varepsilon_2 A / d_2$$

$$\frac{1}{C} = \frac{1}{C_1} + \frac{1}{C_2} = \left(\frac{d_1}{\varepsilon_1} + \frac{d_2}{\varepsilon_2} \right) \frac{1}{A} = \frac{d_1 \varepsilon_2 + d_2 \varepsilon_1}{\varepsilon_1 \varepsilon_2 A}$$

$$C = \frac{\varepsilon_1 \varepsilon_2 A}{\varepsilon_1 d_2 + \varepsilon_2 d_1} = \frac{\varepsilon_{eff} A}{d_1 + d_2}$$

$$\text{where } \varepsilon_{eff} = \frac{\varepsilon_1 \varepsilon_2 \left(d_1 + d_2 \right)}{\varepsilon_1 d_2 + \varepsilon_2 d_1}$$

3.4 Tuning by Means of an Adjustable Air-gap

3.4.2 Effective Permittivity – Heuristic Derivation

- Applying this to the geometry of Fig. 1.19,

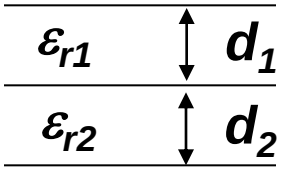

$$\varepsilon_2 = \varepsilon_0, \qquad \varepsilon_1 = \varepsilon_r \varepsilon_0 = \varepsilon, \qquad d_1 = t, \qquad d_2 = \Delta,$$

$$\varepsilon_{eff} = \frac{\varepsilon\varepsilon_0 (t+\Delta)}{\varepsilon_r \varepsilon_0 \Delta + \varepsilon_0 t} = \frac{\varepsilon (t+\Delta)}{(t+\Delta\varepsilon_r)}$$

Since $\varepsilon_r > 1$, $\varepsilon_{eff} < \varepsilon$ when $\Delta > 0$

$\varepsilon_{eff} = \varepsilon$ when $\Delta = 0$

3.4 Tuning by Means of an Adjustable Air-gap

3.4.3 Theoretical and Experimental Results

- The region between the patch and the ground plane is now a two-layer cavity. The microstrip patch antenna with an air-gap can therefore be analyzed using the cavity model. The original assumptions of the cavity model are modified to account for the two-layers as follows:

  (1) Owing to the close proximity between the conducting patch and the ground plane only transverse magnetic (***TM***) modes are assumed to exist. The z-component of the electric field, however, is a function of ***z*** since the cavity is low-layered.

  (2) The cavity is assumed to be bounded by perfect electric walls on the top and on the bottom and by a perfect magnetic wall along the edge.

  (3) Across the dielectric-air interface the tangential electric field and the normal electric flux density are continuous.

3.4 Tuning by Means of an Adjustable Air-gap

3.4.3 Theoretical and Experimental Results

- Based on the previous assumptions, detailed analysis for coaxially-fed circular and annular-ring patches with airgaps were carried out and good agreement between theory and experiment was obtained. The results were summarized in Dahele and Lee [1985].
- In particular, the formula for the resonant frequency is a very simple one and is given by

$$f_{nm}(\Delta) = f(0)\sqrt{\frac{\varepsilon}{\varepsilon_{eff}}}$$

where $f_{nm}(0)$ is the resonant frequency where there is no airgap and ε_{eff} is the effective permittivity of the two-layer medium:

$$\varepsilon_{eff} = \frac{\varepsilon(t+\Delta)}{(t+\Delta\varepsilon_r)}$$

3.4 Tuning by Means of an Adjustable Air-gap

3.4.3 Theoretical and Experimental Results

- Note that the formula for ε_{eff} is identical to the one derived in section B. The formula for $f_{nm}(\Delta)$ is valid for any patch shape. As the airgap width Δ increases, ε_{eff} decreases and the resonant frequency increases. The dependence of $f_{nm}(\Delta)$ on Δ, however, is not a linear one.

3.4 Tuning by Means of an Adjustable Air-gap

3.4.3 Theoretical and Experimental Results

- Results for a coaxially fed circular patch (Lee, Ho, Dahele; 1984)

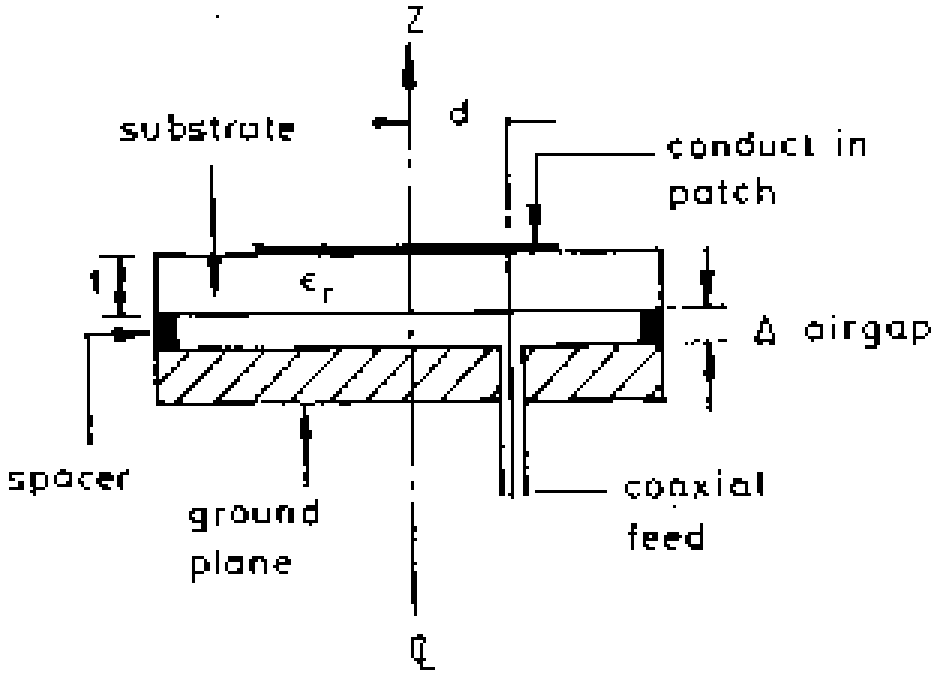

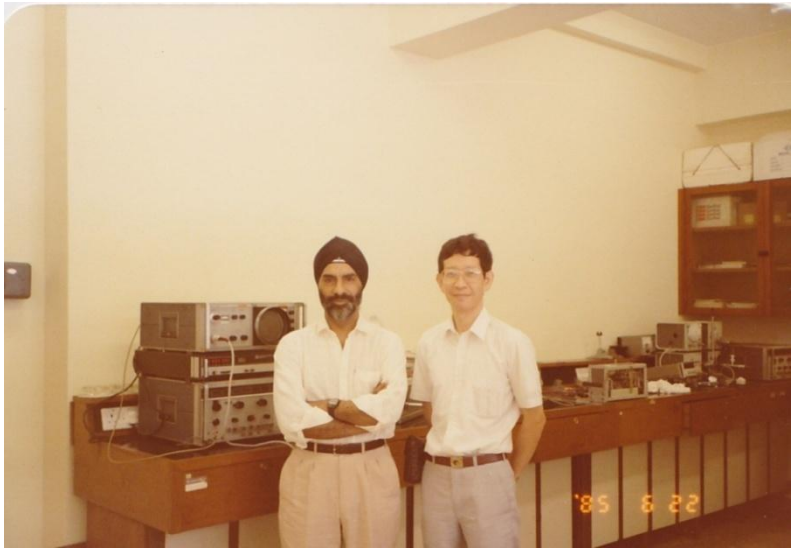

Fig. 1.21 (a) Geometry of the antenna **(b) Dr. J. S. Dahele and Dr. K. F. Lee, CUHK**

3.4 Tuning by Means of an Adjustable Air-gap

3.4.3 Theoretical and Experimental Results

- Results for a circular patch (Lee, Ho, Dahele; 1984):

Table 2.1 Measured resonant frequencies and impedance bandwidths of the first few modes of a 5 cm radius circular-disc antenna with ε_r = 2.32, t = 0.159 cm, fed at 4.75 cm from the center, for three values of the air-gap width Δ.

	Δ = 0		Δ = 0.5 mm		Δ = 1.0 mm	
	f_{nm}	% BW	f_{nm}	% BW	f_{nm}	% BW
TM_{11}	1128 MHz	0.89	1286 MHz	1.48	1350 MHz	2.07
TM_{21}	1879 MHz	0.85	2136 MHz	2.15	2256 MHz	2.61
TM_{31}	2596 MHz	0.77	2951 MHz	1.63	3106 MHz	2.02

3.4 Tuning by Means of an Adjustable Air-gap

3.4.3 Theoretical and Experimental Results

- Results for a circular patch (Lee, Ho, Dahele; 1984):

Table 2.2 Comparison of calculated and measured resonant frequencies for the circular-disc microstrip antennas.

	$\Delta = 0$		$\Delta = 0.5$ mm		$\Delta = 1.0$ mm	
	Calc. **(MHz)**	***Meas.*** **(MHz)**	***Calc.*** **(MHz)**	***Meas.*** **(MHz)**	***Calc.*** **(MHz)**	***Meas.*** **(MHz)**
TM_{11}	1127	1128	1276	1286	1351	1350
TM_{21}	1869	1879	2117	2136	2241	2256
TM_{31}	2571	2596	2911	2951	3082	3106

r = 5.0 cm, t = 0.159 cm, d = 4.75 cm, ε_r = 2.32.

3.4 Tuning by Means of an Adjustable Air-gap

3.4.3 Theoretical and Experimental Results

- Results for a circular patch (Lee, Ho, Dahele; 1984):

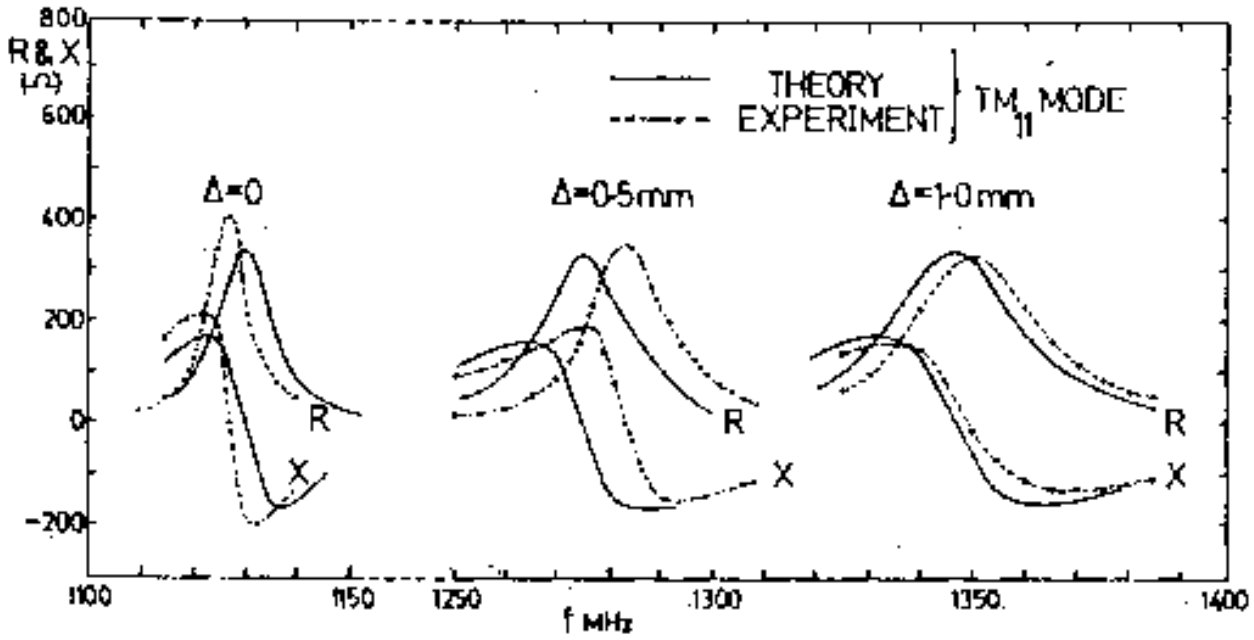

Fig. 1.22

3.4.4 Advantages of Air Gap Tuning

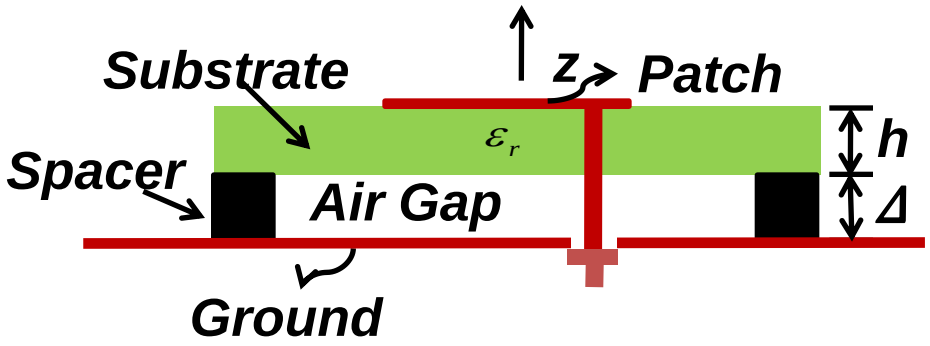

- No need to add components such as varactor diodes or shorting posts and the associated circuitry
- Can be applied to patches of any shape

Problem with probe-feeding

Each time the thickness of the air gap is changed, de-soldering and re-soldering are needed. This not a problem for aperture coupled and stripline fed patches.

3.4.5 Aperture coupled and strip-line fed patches

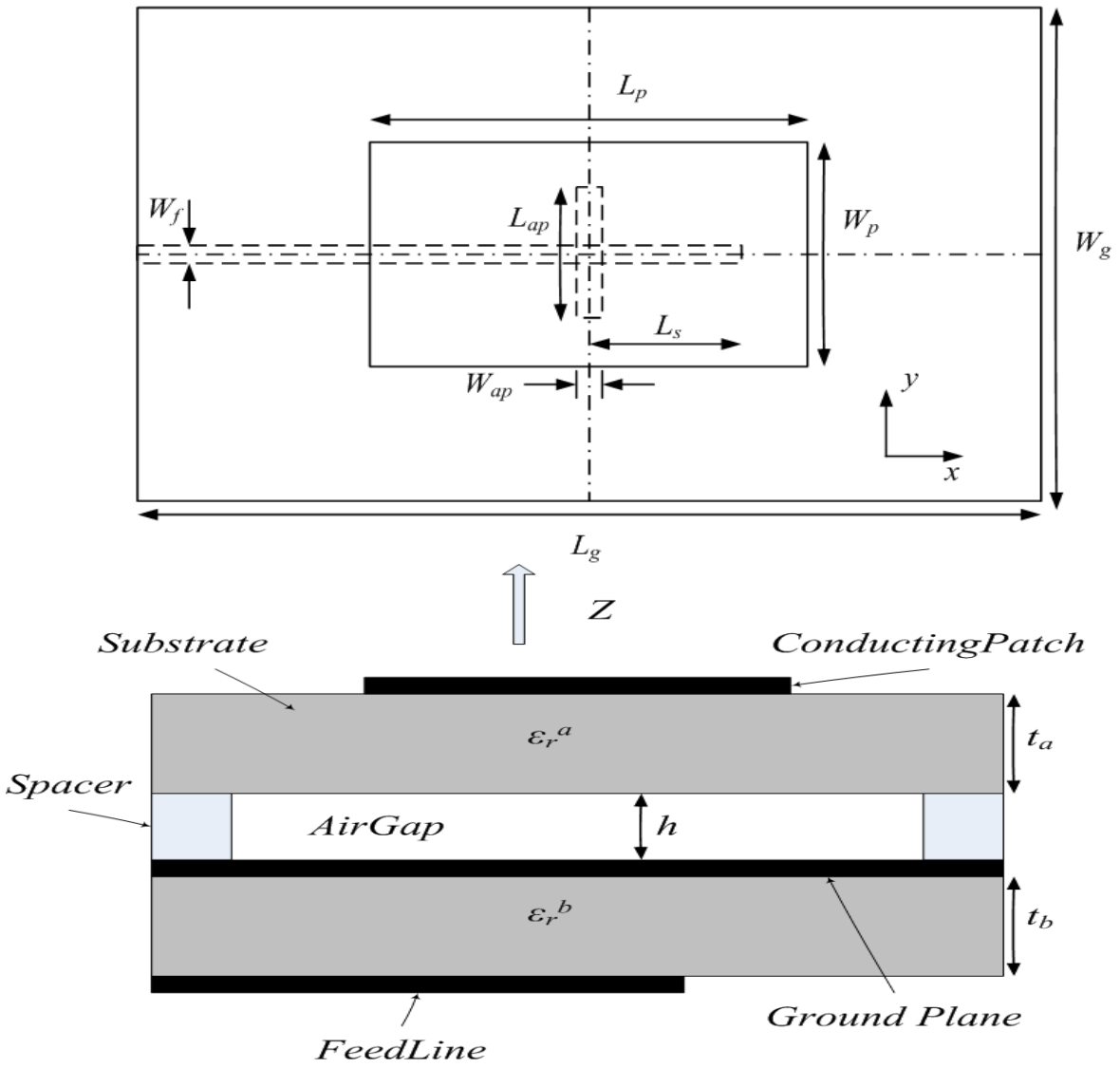

Fig. 1.23 Aperture coupled patch antenna with adjustable airgap

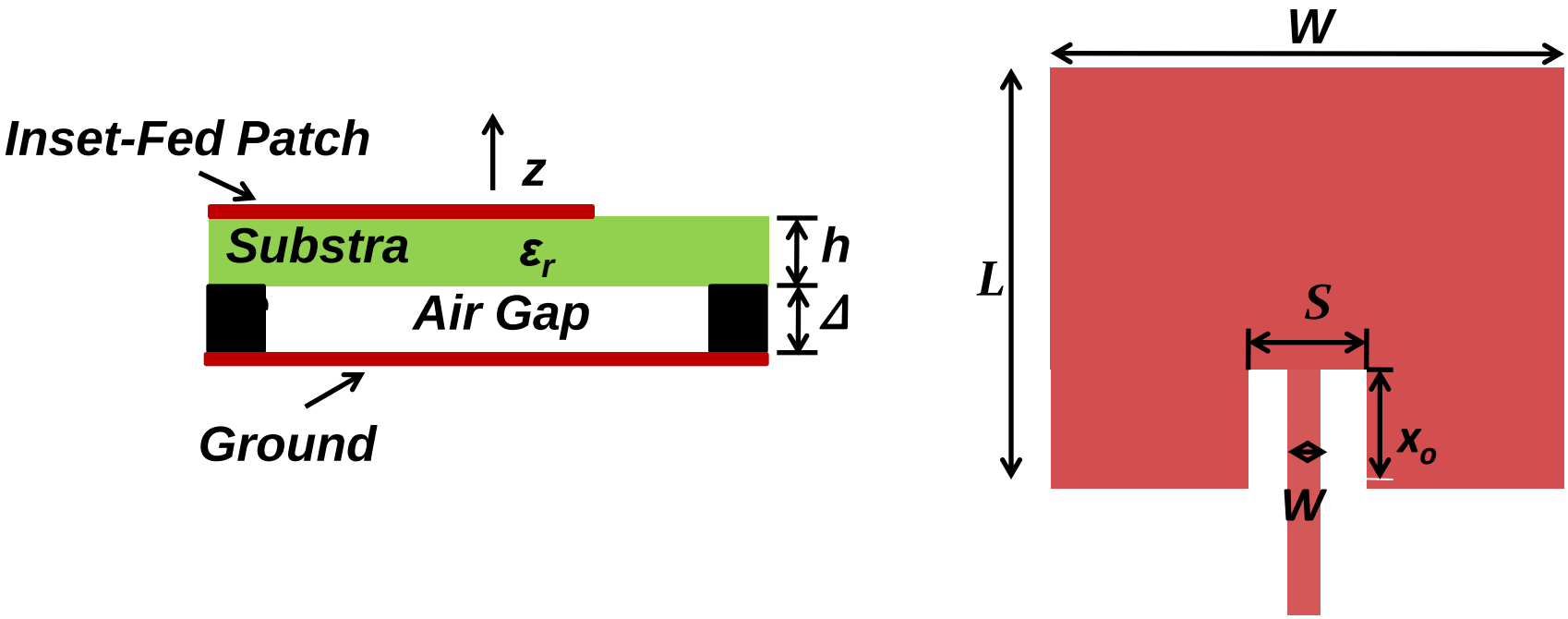

Fig. 1.24 Stripline fed patch antenna with adjustable airgap

- Mao et al. (2011) showed that the adjustable air gap method for tuning the resonant frequency of a patch antenna with aperture-coupled feed and stripline feed is found to be effective. In these cases, changing the air gap width does not require de-soldering and soldering.

- The tuning ranges for coaxial-fed, strip-line fed and aperture-coupled MPA are similar, which is around 20% for $\Delta/h = 0.79$.

- The method is particularly attractive for tuning the resonant frequency of a multi-element patch antenna array fed by aperture coupling or by strip lines. The resonant frequencies of all the elements, and therefore of the array, can be tuned by a single adjustment of the air gap width Δ. This idea, however, remains to be demonstrated.

References on patches with air gap

- P. Bhartia, and I. Bahl, "A frequency agile microstrip antenna," *IEEE AP-S Int. Symp. Digest*, pp. 304-307, 1982.

- D. H. Schaubert, F. G. Farrar, A. R. Sindoris, and S. T. Hayes, "Microstrip antennas with frequency agility and polarization diversity," *IEEE Trans. Antennas Propagat*., Vol. AP-29, pp. 118-123, 1981.

- K. F. Lee, K. Y. Ho, and J. S. Dahele, "Circular-disk microstrip antenna with an air gap," *IEEE Trans. Antennas Propagat*., Vol. AP-32, pp. 880-884, 1984.

- J. S. Dahele, and K. F. Lee, "Theory and experiment on microstrip antennas with airgaps," *IEE Proc*., 132H, pp. 455-460, 1985.

- Yilin Mao, Yashwanth R. Padooru, Kai Fong Lee, A. Z. Elsherbeni, and Fan Yang, "Air gap tuning of patch antenna resonance," 2011 IEEE AP-S/URSI International Symposium Digest, Spokane, Washington

4. Our research on topics related to basic studies

4.1 The annular-ring patch

4.2 The equitriangular patch

4.3 Cross polarization characteristics of rectangular and circular patches

4.4 Patch on cylindrical surface

4.1 The Annular-Ring Patch

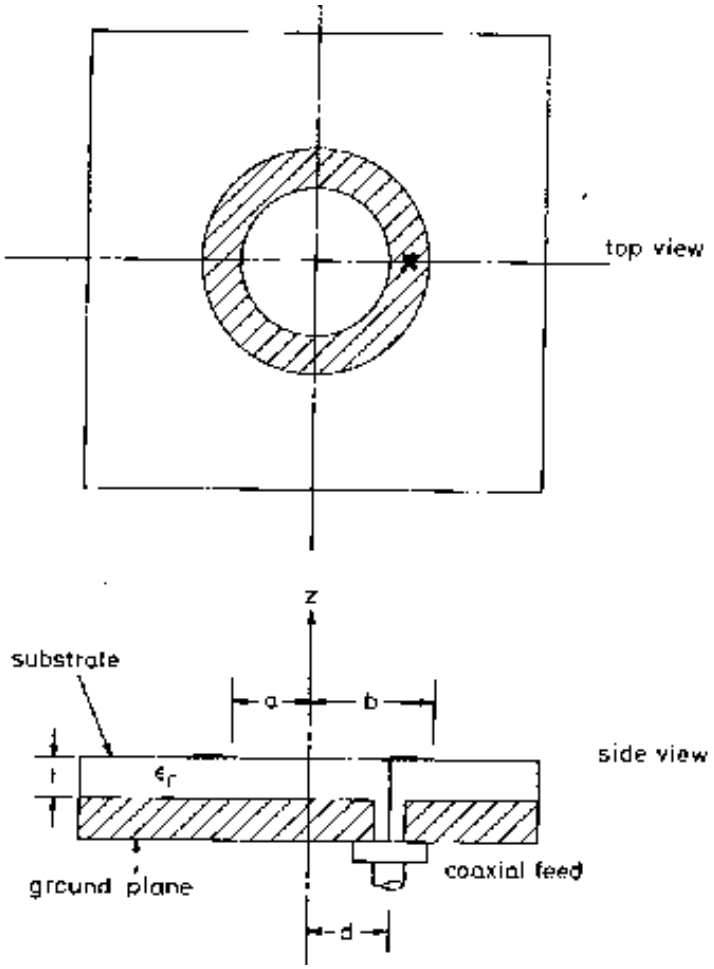

Fig. 1.25 Geometry of the annular-ring patch antenna.

In 1982, W. C. Chew published a full wave analysis of the annular-ring patch antenna. The main findings concerned the two broadside modes: the lowest TM_{11} mode and the higher order TM_{12} mode:

- ***TM_{11} mode***
  - Impedance does not vary much with feed position.
  - Very large resonant resistance; needs matching circuit.
  - Very narrow bandwidth (1% or less).
- ***TM_{12} mode***
  - Impedance sensitive to feed position.
  - With the feed near the inner edge, a good match near 50 Ω can be obtained.
  - For typical parameters used in practice, the bandwidth is about 4 %, which is several times larger than that of the rectangular and circular patches with the same dielectric constant and thickness.

Broadside Modes TM_{11} and TM_{12}

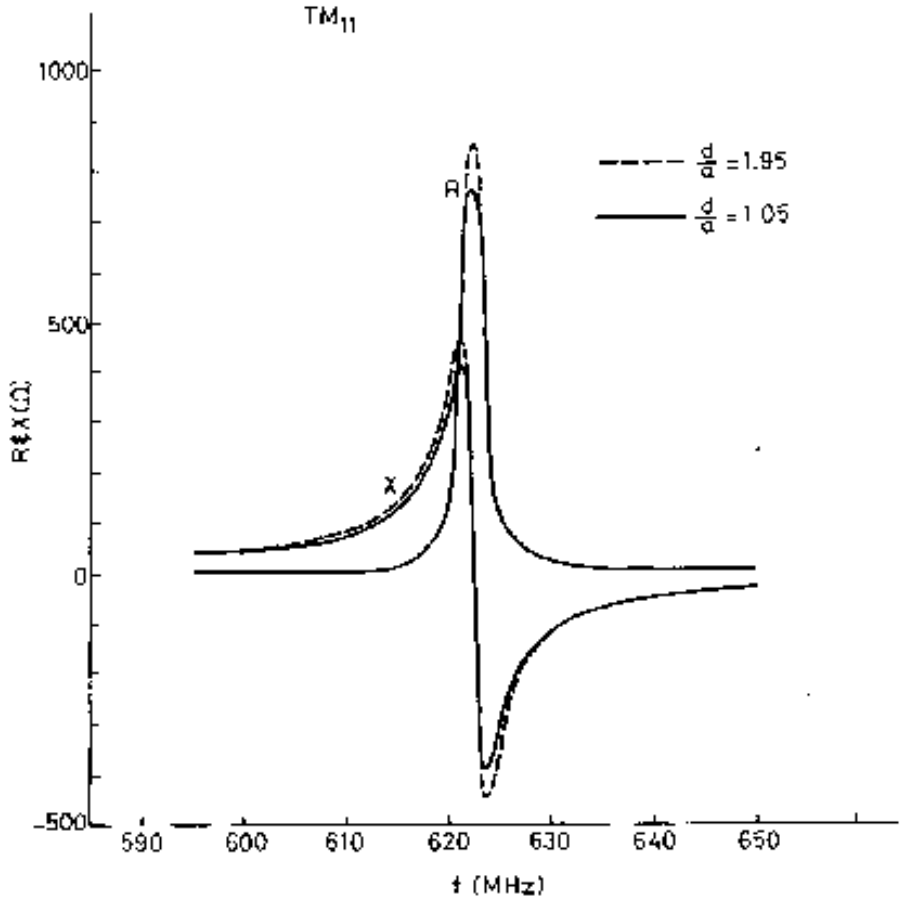

Fig. 1.26 Theoretical input impedance of the *TM*$_{11}$ mode of an annular-ring patch antenna with *b* = 7.0 cm, *a* = 3.5 cm, ε_r = 2.32, *t* = 0.159 cm, fed at two radial locations.

Broadside Modes TM_{11} and TM_{12}

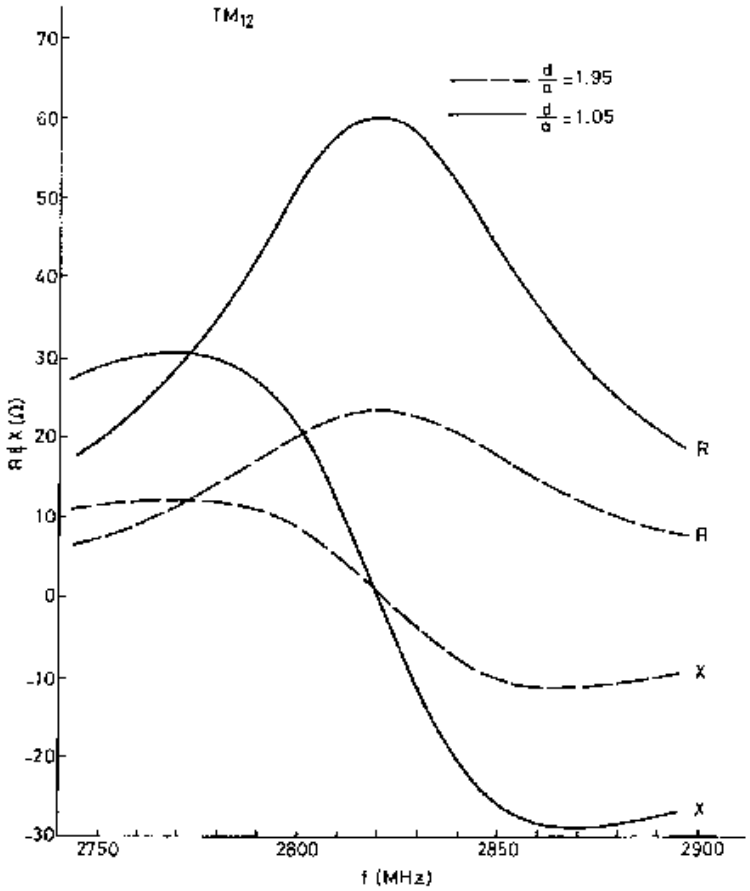

Fig. 1.27 Theoretical input impedance of the *TM*$_{12}$ mode of an annular-ring patch antenna with *b* = 7.0 cm, *a* = 3.5 cm, ε_r = 2.32, *t* = 0.159 cm, fed at two radial locations.

Upon seeing Chew's paper, Dr. Jash Dahele and I fabricated an annular-ring patch antenna and performed the measurements on the TM_{11} and TM_{12} modes. The predictions were verified. We submitted the results to Electronics Letters, which published them in an issue in November 1982, the same year that Chew's paper was published. We received a letter from Chew congratulating us and expressing his appreciation that his theoretical predictions were verified experimentally.

However, the excitement that the TM_{12} mode of the annular-ring patch can provide a bandwidth of some 4 percent did not last long. First, this was achieved at the expense of increasing the size of the patch (for the same operating frequency). Second, subsequent bandwidth broadening techniques obtained much better improvement than can be obtained by the use of the TM_{12} mode.

4.2 The Equitriangular Patch

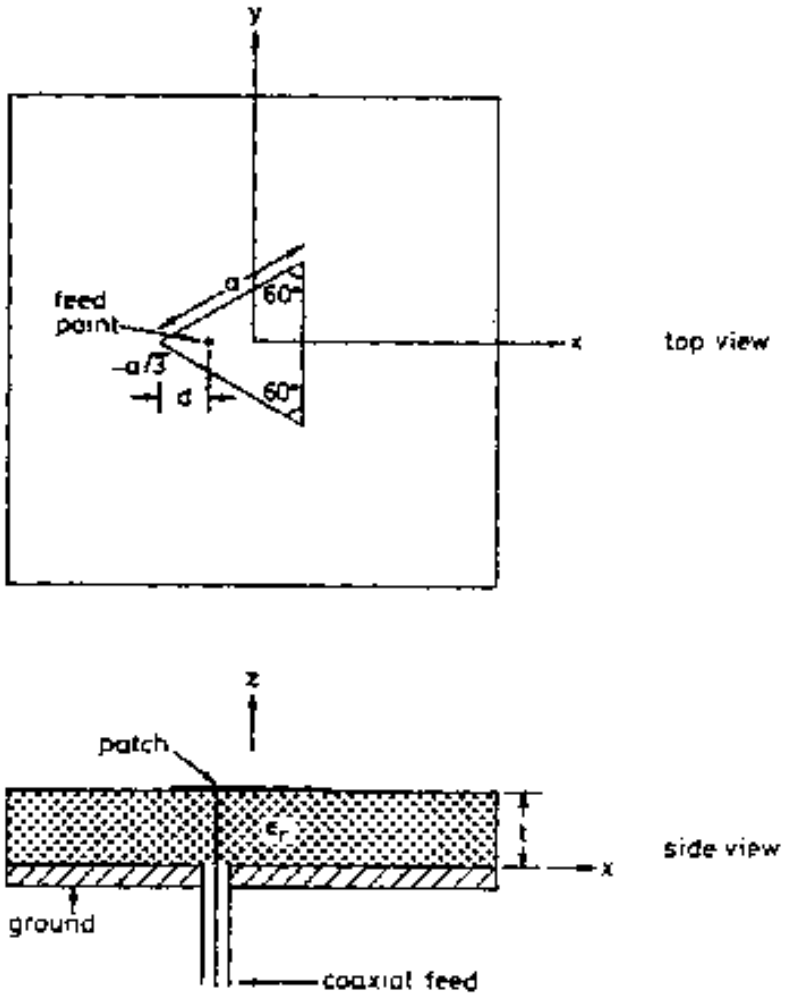

Fig. 1.28 Geometry of the equitriangular patch antenna.

Our contributions:

A. **Accurate measurement of resonant frequencies**
B. **Developed a CAD (computer aided design) formula for the resonant frequencies**
C. **A comprehensive cavity model theory for the equitriangular patch, with experimental verification**

Table 2.3 Measured resonant frequencies of the first five modes of an equilateral triangular patch antenna with a=10 cm, ε_r=2.32, and thickness 0.159 cm. (Dahele and Lee 1987)

Mode	Measured f_{mn} (MHz)
TM_{10}	1280
TM_{11}	2240
TM_{20}	2550
TM_{21}	3400
TM_{30}	3824

Theoretical Resonant Frequency from Cavity Model assuming a perfect magnetic wall:

$$f_{mn} = \frac{ck_{mn}}{2\pi\sqrt{\varepsilon_r}} = \frac{2c}{3a\sqrt{\varepsilon_r}}\left(m^2 + mn + n^2\right)^{\frac{1}{2}}$$

Question: What correction factor(s) to use to account for the fringing fields and the two-layer dielectric?

In the literature, a number of papers were devoted to answer this question, based mainly on guess work. All of them used our measurements to compare their predictions, and to see whether their correction factor(s) are more accurate than those of others.

CAD formula for resonant frequency:

In 1992, Chen, Lee and Dahele, instead of guessing, obtained an expression for the effective sidelength a_e by curve fitting the data results obtained from full-wave analysis using moment method:

$$a_e = a\left[\begin{array}{l} 1+2.199\left(\frac{h}{a}\right)-12.853\left(\frac{1}{\sqrt{\varepsilon_r}}\right)\left(\frac{h}{a}\right) \\ +16.436\left(\frac{1}{\varepsilon_r}\right)\left(\frac{h}{a}\right)+6.182\left(\frac{h}{a}\right)^2-9.802\left(\frac{1}{\sqrt{\varepsilon_r}}\right)\left(\frac{h}{a}\right)^2 \end{array}\right]$$

- Accuracy of this expression is within 1% when compared with the value obtained from moment method analysis and with experiment .
- The comparisons were carried out for ε_r = 2.32, $0.002 \le h/\lambda_0 \le 0.125$ and ε_r = 10.0, $0.008 \le h/\lambda_0 \le 0.032$

When Prof. Luk joined City Polytechnic in June 1985, I asked him to work out a complete cavity-model-based theory for the equitriangular patch antenna. We presented the results in the 1986 AP meeting in Philadelphia, and a paper was published in the AP Transactions in 1988. This paper has become a standard reference on the equitriangular patch antenna.

Prof. K. M. Luk at City Polytechnic in 1985 doing research on the equitriangular patch antenna

Prof. K. M. Luk, Prof. J. S. Dahele and myself at the 1986 AP meeting in Philadelphia, where the paper on the equitriangular patch was presented

4.3 Cross-Polarization Characteristics of rectangular and circular patches

- If a rectangular patch is excited at the resonant frequency of the TM_{01} mode, the dominant contribution to the cross-polarized field is the TM_{10} mode. The higher order TM_{m0} modes also contribute, but they will be much weaker than that of the TM_{10} mode.

- The ratio of co-polarization to cross polarization in a particular direction is approximately given by $|E_{01}(\theta,\phi)|/|E_{10}(\theta,\phi)|$. Similarly, if the patch is excited at the resonant frequency of the TM_{10} mode, it is given approximately by $|E_{10}(\theta,\phi)|/|E_{01}(\theta,\phi)|$. For the first case, Oberhart *et al*. (1989) showed that the cross-polarization level is dependent on ***a/b***. For a patch fed at the $x' = 0$ edge, the cross-polarization is smallest when ***a/b*** = 1.5, about 21dB below the co-polarized field.

- Extensive studies showing how the co-polarized to cross-polarized ratios depend on substrate thickness, feed position and resonant frequencies, are given by Huynh, Lee and Lee (1988) based on the cavity model.

- A similar study for the circular patch was carried out using the cavity model by Lee, Luk and Tam in 1992.

- For the rectangular patch, further study using simulation software and performing measurements, was done by Yang, Lee and Luk in 2008.

over ordinary telephone lines'. Image Sequence Processing and Dynamic Scene Analysis *in* NATO ASI series, 1983, pp. 314–336
3 ROSENFELD, A., and KAK, A. C.: 'Digital picture processing', vol. 2 (Academic Press, New York, 1982)
4 SHIOJAKI, A.: 'Edge extraction using entropy operator', *Comput. Vision, Graphic. & Image Process.*, 1986, **36**, pp. 1–9

CROSSPOLARISATION CHARACTERISTICS OF RECTANGULAR PATCH ANTENNAS

Indexing terms: Antennas, Microstrip, Antenna theory

Theoretical results describing the crosspolarisation characteristics of rectangular patch antennas are presented. Of particular interest is the result that the copolarisation radiation is not sensitive to resonant frequency and substrate thickness while the crosspolarisation component increases with resonant frequency and/or substrate thickness.

Introduction: Although the crosspolarisation characteristic is an important consideration in the design of microstrip antennas, few detailed theoretical results are available in the literature. Oberhart *et al.*[1] recently discussed the quantity $|E_{copol}|/|E_{xpol}|$ of a rectangular patch excited in the TM_{01} mode and showed that it is dependent on the aspect ratio a/b. In this letter, we present detailed results showing the variation of this quantity for different feed positions, substrate thicknesses, and resonant frequencies.

Theory: Following Reference 1, we based our calculations on the cavity model. Let the substrate relative permittivity be ε_r, thickness t, and dimensions a and b, with $a > b$. The coaxial feed is located at (x', y') and is modelled by a current ribbon of width d. For a current of 1 A, the magnitudes of E_θ and E_ϕ in the far-zone consist of an infinite sum of modes:

$$|E_\theta| = C\psi_1 \cos\phi \sum_{m,n=0}^{\infty} \varepsilon_{om}\varepsilon_{on} \sin\left[\tfrac{1}{2}(k_0 b\psi_1 - n\pi)\right] \times \sin\left[\tfrac{1}{2}(k_0 a\psi_2 - m\pi)\right] \cdot j_0\left(\frac{m\pi d}{2a}\right) \times \left[\frac{1}{k_0^2\psi_2^2 - \left(\frac{m\pi}{a}\right)^2} + \frac{1}{k_0^2\psi_1^2 - \left(\frac{n\pi}{b}\right)^2}\right] \times \frac{\cos\left(\frac{m\pi x'}{a}\right)\cos\left(\frac{n\pi y'}{b}\right)}{(k^2 - k_{mn}^2)} \quad (1)$$

Let the magnitude of the electric field corresponding to mode (m, n) be E_{mn}. If the patch is excited at the resonant frequency of the TM_{01} mode, the ratio of copolarisation to crosspolarisation in a particular direction is given by $|E_{01}(\theta, \phi)|/|\sum E_{mn}(\theta, \phi)|$. Similarly, if the patch is excited at the resonant frequency of the TM_{10} mode, it is given by $|E_{10}(\theta, \phi)|/|\sum E_{on}(\theta, \phi)|$. In the next Section, some numerical results showing the dependence of $|E_{01}(\theta, \phi)|/|\sum E_{mn}(\theta, \phi)|$ on resonant frequency will be given for different substrate thicknesses and feed positions along the edges. For brevity, only the case corresponding to $\varepsilon_r = 2{\cdot}32$ and $a/b = 1{\cdot}5$ is presented.

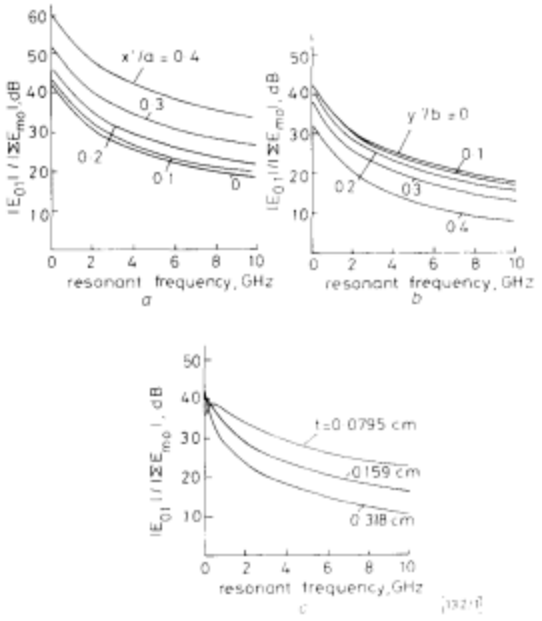

Fig. 1

a $|E_{01}|/|\sum E_{mn}|$ in broadside direction as a function of resonant frequency for different feed positions along side a ($\varepsilon_r = 2{\cdot}32$, $t = 0{\cdot}159$ cm, $a = 1{\cdot}5b$, $y'/b = 0$)
b $|E_{01}|/|\sum E_{mn}|$ in broadside direction as a function of resonant frequency for different feed positions along side b ($\varepsilon_r = 2{\cdot}32$, $t = 0{\cdot}159$ cm, $a = 1{\cdot}5b$, $x'/b = 0$)
c $|E_{01}|/|\sum E_{mn}|$ in broadside direction as a function of resonant frequency for three substrate thicknesses ($\varepsilon_r = 2{\cdot}32$, $a = 1{\cdot}5b$, $x'/a = 0$, $y'/b = 0{\cdot}2$)

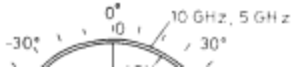

4.4 Patch on cylindrical surface

One of the advantages of patch antennas is that they can be mounted on curved surfaces. Example:

Microstrip array on wing shape Air Force Research Lab. Hanscom AFB, USA

We published one of the early papers on patch antennas on cylindrical surfaces in 1989. The theory was worked out by Prof. Luk at City Polytechnic and experimental work was done by Prof. J. S. Dahele at the Royal Military College of Science.

Experiment on patch on cylindrical surface was performed by Dr. J. S. Dahele at the Royal Military College of Science, Shrivenham, UK

IEEE TRANSACTIONS ON ANTENNAS AND PROPAGATION, VOL. 37, NO. 2, FEBRUARY 1989

Analysis of the Cylindrical-Rectangular Patch Antenna

KWAI-MAN LUK, MEMBER, IEEE, KAI-FONG LEE, SENIOR MEMBER, IEEE, AND JASHWANT S. DAHELE, SENIOR MEMBER, IEEE

Abstract—**A comprehensive analysis of a thin cylindrical-rectangular microstrip patch antenna which includes resonant frequencies, radiation patterns, input impedances and Q factors is presented. Numerical and graphical results are given to illustrate the effects of curvature on the characteristics of the TM_{10} and TM_{01} modes.**

I. Introduction

ONE OF THE MAJOR advantages of microstrip patch antennas is that they can be made conformal to the surfaces on which they are mounted. For example, rectangular patches are often mounted on cylindrical surfaces. Such rectangular-cylindrical microstrip patch antennas have been the subject of several investigations. Krowne [1] calculated the resonant frequencies while Wu *et al.* [2] and Ashkenazy *et al.* [3] calculated the radiation patterns. In [2] the cavity model was used in conjunction with the method of images, but the

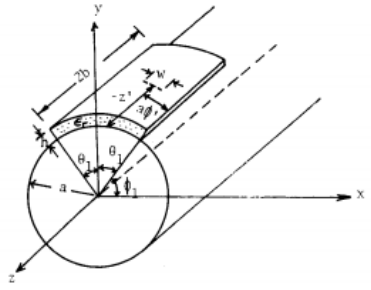

Fig. 1. Geometry of the cylindrical-rectangular microstrip patch antenna.

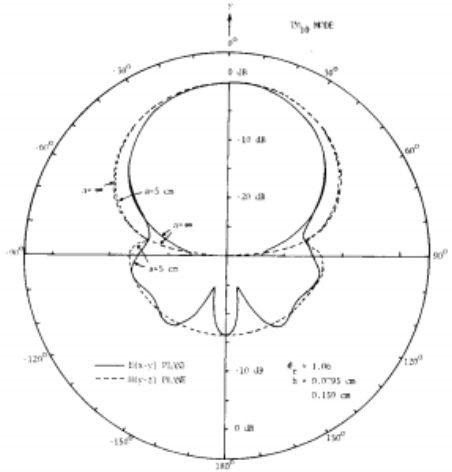

Fig. 2. Power patterns in the $E(x-y)$ and $H(y-z)$ planes for the TM_{10} mode with $\epsilon_r = 1.06$.

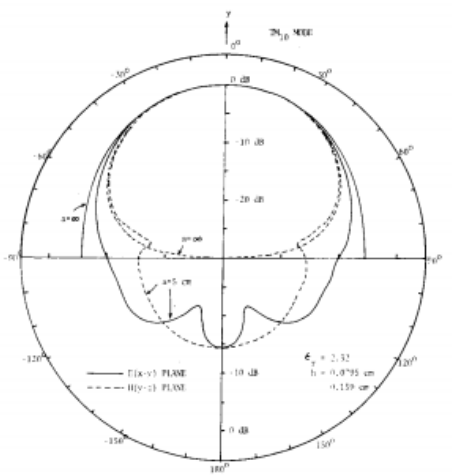

Fig. 3. Power patterns in the $E(x-y)$ and $H(y-z)$ planes for the TM_{10} mode with $\epsilon_r = 2.32$.

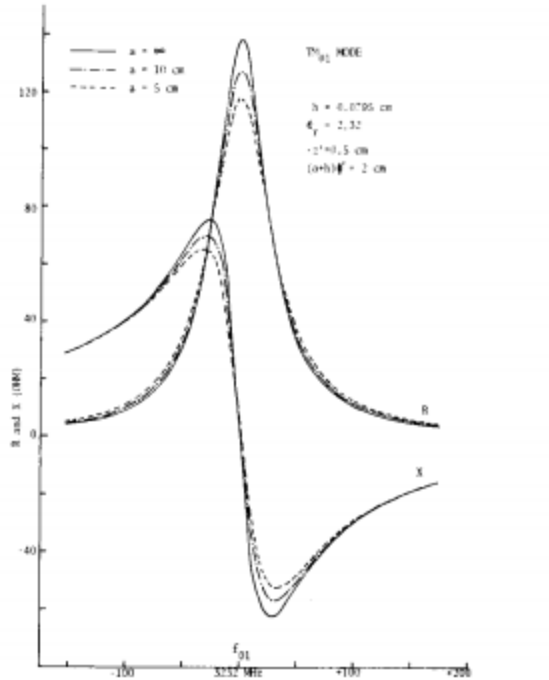

Fig. 7. Input impedance of the TM_{01} mode for a curved patch with $2(a + h)\theta_1 = 4$ cm, $2b = 3$ cm and fed at $-z' = 0.5$ cm, $(a + h)\phi' = 2$ cm. $w = 5$ mm, $\epsilon_r = 2.32$, $h = 0.0795$ cm.

Section 4 References

W. C. Chew, "A broad-band annular-ring microstrip antenna," *IEEE Trans. Antennas Propagat*., Vol. AP-30, pp. 918-922, 1982.

J. S. Dahele and K. F. Lee, Characteristics of annular-ring microstrip antenna, Electronics Letters, 18, 1051-1052, 1982.

K. F. Lee, K. M. Luk, and J. S. Dahele, "Characteristics of the equilateral triangular patch antenna," *IEEE Trans. Antennas Propagat*., Vol. AP-36, pp. 1510-1518, 1988.

J. S. Dahele, and K. F. Lee, "On the resonant frequencies of the triangular patch antenna," *IEEE Trans. Antennas Propagat*., Vol. AP-32, pp. 100-101, 1987.

W. Chen, K. F. Lee, and J. S. Dahele, "Theoretical and experimental studies of the equilateral triangular patch antenna," *IEEE Trans. Antennas Propagat*., Vol. AP-40, pp. 1253-1256, 1992.

M. L. Oberhart, Y. T. Lo, and R. Q. H. Lee, "New simple feed network for an array module of four microstrip elements," *Electron. Lett*. Vol. 23, pp. 436-437, 1987.

T. Huynh, K. F. Lee and R. Q. Lee, Cross polarization characteristics of rectangular patch antennas, Electronics Letters, Vol. 24, 463-464, 1988.

K.M. Luk, K. F. Lee & J. S. Dahele, Analysis of the cylindrical-rectangular microstrip antenna, IEEE Transactions on Antennas and Propagation, AP-37, 143-147, 1989.

S. L. S. Yang, K. F. Lee, A. A. Kishk and K. M. Luk, "Cross Polarization Studies of rectangular patch antenna," Microwave and Optical Technology Letters, Vol. 50, pp. 2099-2103, 2008.